the eyes of their children. For far more advanced disease in which tumor spread toward anterior structures of the eye or infiltrates into the optic disc, and if a massive hemorrhage was developed in retina or vitreous space with a loss of vision, enucleation was employed with or without systemic chemotherapy according to the pathological risk features. Systemic chemotherapy regimen mostly used in this cohort was 3-drug chemotherapy with carboplatin, etoposide, and vincristine.

Tumor response to the preceding therapies was defined as follows. The tumor whose stage attained down-grouping was classified as a good response, up-grouping as a poor response, and no group change as stable.

All episcleral ^{106}Ru plaque applicators (BEBIG Isotopen und Medizintechnik GmbH, Berlin, Germany) were inserted under general anesthesia. Before the operation, tumor location and height were assessed by slit lamp examinations with or without ultrasound and an appropriate plaque was selected. The plaques are hemispherically shaped with radii of 12 and 14 mm. CIA and CIB are used to treat anteriorly located tumor because they are semicircularly shaped concave in order to avoid cornea. COC are used to treat the tumor located in the posterior pole with a notch to avoid optic disc. CCA and CCB are round shaped and used to treat tumors which are away from cornea or optic disc. The diameters of A and B are 15.5 mm and 20 mm, respectively. To insert the plaques, extraocular muscles were separated temporarily. The selected plaques were sutured through the plaque eyelets to the sclera surface. The plaques were removed also under general anesthesia after the planned duration of radiation. The duration of radiation was calculated to administer prescription dose of 40 Gy to the reference depth. The reference depth was the height of tumor plus sclera thickness (1 mm) with a safety margin of 1 mm. Lateral tumor margin was set to 2-3 mm (10). Before July 2005, reliable ultrasound was not available to determine tumor height; therefore, the slit lamp was used to estimate it using its focus. Therefore before July 2005, only tumor width expressed by disc diameter (DD) and reference depths diagnosed approximately by slit lamp were available in the medical records. And for tumors with vitreous seeding, reference depth was set to 5-6 mm, which was regarded as the limit of the range of RPT. Hence, tumors with vitreous seeding without description of reference depth in medical record could be recalculated as having a reference depth of 5-6 mm. Before September 2006, the reference depth was 5 mm and thereafter it was set to 6 mm because of the dose tables provided by the manufacturer. Since May 2002, BEBIG has delivered its ^{106}Ru eye plaques with new protocols of radioactivity measurements in accordance with the National Institute of Standards and Technology calibration system. Therefore recalculations were performed for this study to correct the prescribed dose before the introduction of the new calibration system by using the conversion factor table provided by BEBIG (14). Because most of the conversion factors, which differ by applicator type and reference depth, were greater than 1.0, median dose at the reference depth became greater than 40 Gy after the recalculation (Table 2).

Because the biological effect of RPT could differ by dose rate and combined effect with EBRT must be considered, biologically effective dose (BED) was calculated according to the method of Dale (15) and is given by

$$\mathrm{BED} = \text{Total dose} \times 1 + \frac{2R}{\mu}\left(\frac{\beta}{\alpha}\right)\{1 - 1/\mu T[1 - \exp(-\mu T)]\}$$

where R indicates dose rate, T the treatment time, and μ the repair rate constant of sublethal damage. The value of μ was assumed as 0.46 hour^{-1} (corresponding to repair half time of 1.5 hours) (15). The α/β values used in this analysis were $\alpha/\beta = 10$ Gy for tumor control and $\alpha/\beta = 3$ Gy for late normal tissue morbidities. In 85 of 101 RPTs, the reference depth and prescribed dose could be obtained and BED_{10} (BED with an α/β ratio of 10 Gy) could be calculated. Because the outer surface of the sclera directly touches the plaque applicator (depth 0 mm), dose and BED_3 (BED with an α/β ratio of 3 Gy) of the outer surface of sclera could be calculated for 97 procedures whose applicator type and treatment time were known. For deriving total BED_3 of outer surface of sclera, BED_3 of EBRT, if any, before and after the RPT was added. In 16 eyes in which part of retina had overlapping multiple RPTs, BED_3 of outer surface of sclera of each RPT was added.

Ophthalmologic follow-up was performed with examinations under anesthesia every 1-2 months after the therapy until tumor control was achieved. Thereafter, examinations were performed every 2-6 months as needed.

The probabilities of local control rate (LCR), ocular retention rate (ORR), and overall survival (OS) were calculated using the Kaplan-Meyer method (16). For LCR, 101 tumors treated by 101 RPTs were taken into account. Local control was assessed by retinal diagram before and after the RPTs. Tumor persistent or regrowing within margins of the retina covered by the plaque applicator was considered as local failure. For the estimate of ORR, enucleation from disease progression or treatment-related complications and death from any causes were scored as an event and 90 eyes were subjects of the analysis. ORR was calculated from date of the last RPT to date of the events or to the last follow-up. The relationships between clinical and treatment variables and LCR were analyzed by the univariate and multivariate analyses. A P value of $<.05$ was considered statistically significant. The continuous variables were dichotomized to give the lowest P values in the log-rank test. The variables with P values $<.05$ were further analyzed in multivariate analysis by Cox proportional hazards test.

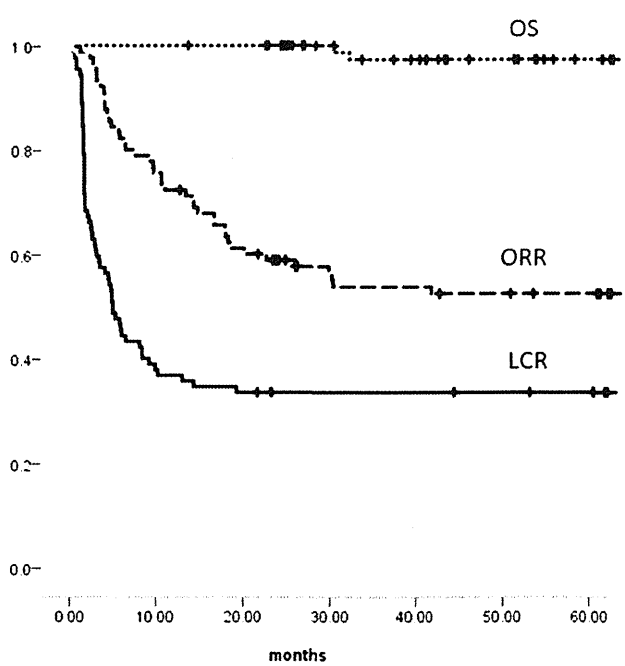

Fig. 1. Kaplan-Meyer curves of local control rate (LCR), ocular retention rate (ORR), and overall survival (OS).

Results

Tumor and treatment characteristics at the 101 RPTs were summarized in Table 2. Median patient follow-up length was 72.8 months (range 12.2-130). LCR of the 101 tumors treated by the 101 RPTs was 33.7% in 2 years with 31 tumors controlled (Fig. 1). All local failures were seen within 24 months after RPTs. The locally failed tumors were managed by various modalities including repeated RPT. Forty-two eyes (46.7%) were enucleated during the follow-up period and estimated 2 and 4 years ORR rates are 58.7% and 52.2%, respectively (Fig. 1).

Univariate analysis revealed clinical and treatment factors related with LCR (Table 3). Unilateral disease, ICRB group C or more at the presentation or at the time of RPT and vitreous seeding/subretinal seedings at the time of RPT, tumor size greater than 5 DD, dose at the reference depth lower than 35 Gy, BED_{10} for the reference depth lower than 40 Gy_{10}, reference depth greater than 5 mm, and dose rate at reference depth lower than 0.7 Gy/hour were associated with unfavorable LCR. Multivariate analysis revealed that ICRB group C or more at the initial presentation or at the time of RPT, and BED_{10} for the reference depth tumor lower than 40 Gy_{10} were statistically significant predictive factors for unfavorable LCR (Table 3). The tumors were classified into 2 groups according to the ICRB and BED_{10} for reference depth (BED_{10}). Group 1 was defined as ICRB A/B both at initial presentation and at RPT and BED_{10} for the reference depth $\geqq 40$ Gy_{10}. All other tumors were classified into group 2. There were 17 tumors in group 1 and 71 in group 2. Sixteen RPTs and 5 tumors lack the information of reference depth and initial ICRB, respectively. But if the tumor ICRB was not A/B at the time of RPT, it could be classified as group 2 even if neither reference depth nor initial ICRB were unknown. Therefore total number included in this grouping was above 85 but below 101. Two-year LCR were 64.7% and 25.4% in group 1 and group 2, respectively, with a statistical significant difference (Fig. 2). During the follow-up period, 2 patients died of brain metastasis with 3-year OS rate of 97.3% (Fig. 1).

As for morbidities, in 1 case, sclera ruptured during the operation, which required systemic chemotherapy but resulted in chemotherapy-refractory relapse and eventual enucleation. Twelve eyes (13.3%) developed retinal detachment, 6 eyes (6.7%) proliferative retinopathy, and 2 eyes (2.2%) rubeosis with abnormal neovascularization of iris. Both eyes with rubeosis eventually were enucleated because of glaucoma or disease progression. Twenty-three (25.6%) of 90 eyes developed posterior subcapsular cataract and 6 eyes required surgery for cataract. Median interval to cataract development after RPT was 35.0 months (range 0-87.33). Posterior subcapsular cataract development related only with whether or not EBRT was performed during the entire clinical course with cataract occurring in 28.1% of the patients undergoing EBRT at 3 years and 2.9% of those without EBRT ($P=.033$) (Fig. 3a). Thirty-four eyes (37.8%) had a retinal and vitreous hemorrhage after RPT. The incidence of retinal detachment, proliferative retinopathy, and rubeosis showed a correlation with radiation dose of the outer surface of sclera. $BED_3 \geqq 1200$ Gy_3 of the outer surface of sclera was significantly associated with a higher incidence either of retinal detachment, proliferative retinopathy or rubeosis ($P=.017$) (Fig. 3b).

There were 2 enucleations without tumor progression—1 of which developed after circulatory collapse of the retina after repeated selective ophthalmic arterial infusions (17) and transpupillary thermotherapy (18) for posterior pole of the retina. The other developed rubeosis iris caused by RPT as mentioned previously.

Two patients had a second malignancy after RPT. Both patients had hereditary retinoblastoma and 1 had family history of retinoblastoma. Both patients received EBRT and 1 had also received chemotherapy. One patient developed rhabdomyosarcoma in the nasal cavity within EBRT radiation field 27 months after the EBRT and 6 months after the RPT. The other had Ewing sarcoma in right mandible outside of EBRT fields 89 months after the EBRT and 76 months after RPT.

Discussion

In this study, we reported treatment results for RPTs for 101 retinoblastomas in 90 eyes of 85 patients in 10 years.

LCR of EBRT was reported to be 31%-64% (19, 20). Although small tumors could be controlled by 40-46 Gy of conventional fractionated EBRT, the control rate of greater tumors was unsatisfactory. Recently, 2 retrospective studies of RPT for retinoblastoma have been published (8, 9). Schueler et al (8) achieved excellent results of 92.9% LCR and eyes could be preserved in 88.6%. Abouzeid et al (9) also showed good results of 59%-73% eye preservation rate. Another radionuclide of ^{125}I also attained an excellent LCR ranging between 83% and 95% (6, 7). The prescribed dose of ^{125}I plaque brachytherapy was 40 Gy (6, 7) but those of RPT has not yet been standardized. In the study of Schueler et al (8) using the National Institute of Standards and Technology dosimetry standard, the dose at the apex ranged from 53-233 Gy and a mean dose extended up to 138 Gy with an estimated accuracy of no better than $\pm 35\%$. They concluded that the recommended dose should be 88 Gy at the tumor apex, although they mentioned the possibility of dose de-escalation (8). On the other hand, Abouzeid et al (9) prescribed 50 Gy at the tumor apex and found that the apical dose was not a predictive factor of local failure. They concluded that favorable tumor control could be achieved with a median dose at the tumor apex of 51.7 Gy. In this study, recalculated median dose at the tumor apex was 47.4 Gy (range 24.3-86.1 Gy) and comparable to that of Abouzeid et al (9). However, 2-year LCR of the current study was 33.7% and inferior to the other studies of RPT. The unfavorable LCR can be explained by the facts that 62.3% of the patients belonged to ICRB group C or more with unfavorable factors of vitreous seeding or subretinal seedings in the current study. In contrast, other studies included only the patients with tumors up to ICRB group C with a limited vitreous seedings. However, it has to be emphasized that as shown in Table 3, even with the presence of vitreous seedings about 20% of tumors could be controlled by RPT. Although tumor control rate of RPT with unfavorable factors were dismal, progressed tumors could be ultimately salvaged by enucleation without risking survival; therefore, it is meaningful to try to treat advanced tumors with a conservative approach including RPT especially for the patients whose contralateral eye had already been enucleated. As shown in Fig. 2, LCR for tumors without unfavorable factors were comparable to the other series (8, 9).

Factors that influenced LCR were disease laterality, ICRB, vitreous/subretinal seeding, tumor size, reference depth, dose, and dose rate at reference depth. It was in accordance with other reports that pointed out that vitreous seeding, subretinal seeding, and dose at the tumor apex were prognostic factors of local

Table 3 Univariate and multivariate analysis of potential predictive factors influencing LCR*

	LCR				
Factors	2-y	*P* value in uni	*P* value in multi	Hazard ratio	95% CI
Gender					
Male	36.2	.462			
Female	29.4				
Laterality					
Bilateral	38.9	.017*	.133		
Unilateral	15.0				
ICRB at initial presentation					
Group A/B	53.3	.022*	.001*	10.323	2.737 38.932
Group C/D/E	24.1				
ICRB at brachytherapy					
Group A/B	55.9	<.001*	.027*	0.441	0.213 0.911
Group C/D/E	20.7				
Applicator type					
CIA/CCA	42.1	.141			
CIB/CCB	26.0				
Prior EBRT					
Yes	32.0	.707			
No	35.7				
Treatment type					
First-line/second-line	27.1	.152			
Salvage	45.5				
Vitreous seeding at brachytherapy					
Yes	18.9	.016*	.892		
No	43.6				
Subretinal seeding at brachytherapy					
Yes	19.2	.04*	.785		
No	39.4				
Response to preceding therapy					
Good	43.8	.116			
Stable/poor	28.6				
Tumor size at brachytherapy (DD)					
<5 DD	52.5	.001*	.252		
≧5 DD	19.6				
Dose rate at outer surface of sclera					
<3 Gy/h	29.5	.271			
≧3 Gy/h	36.4				
Reference depth					
<5 mm	47.1	.01*	.295		
≧5 mm	21.4				
Dose rate at reference depth					
<0.7 Gy/h	17.9	.011*	.105		
≧0.7 Gy/h	40.4				
Dose at reference depth (Gy)					
<35 Gy	11.8	.008*	.448		
≧35 Gy	37.9				
Dose at reference depth (BED_{10})					
<40 Gy_{10}	0.0	.001*	.034*	2.237	1.063 4.710
≧40 Gy_{10}	36.9				
Treatment time					
<53 h	37.8	.195			
≧53 h	29.8				

Abbreviations: BED = biological effective dose; CI = confidence interval; DD = disc diameter; EBRT = external beam radiation therapy; ICRB = the International Classification of Retinoblastoma; LCR = local control rate; multi = multivariate analysis; uni = univariate analysis.

* $P<.05$.

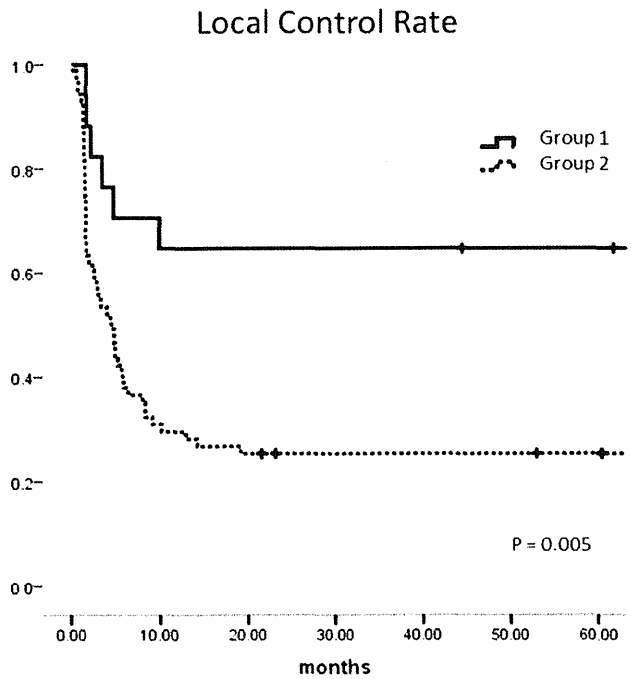

Fig. 2. Local control rate (LCR) according to the group classification by the International Classification of Retinoblastoma and biological effective dose (BED) with $\alpha/\beta = 10$ Gy of the reference depth (for details refer to the text).

control. Both reference depth and dose rate at reference depth were prognostic factors of local control suggesting that physical limitation of RPT, which is not suitable for treating tall tumors as previously reported (8-11).

The administration of previous EBRT did not influence LCR (Table 3), suggesting that response to RPT did not differ between relapsed or refractory tumors after EBRT and radiation-naive tumors as previously reported (9).

Concerning the morbidities, the incidence of posterior subcapsular cataract was influenced by EBRT but not by RPT whose dose to the lens is negligible. In the current study, the incidence of proliferative retinopathy was as low as 6.7%, which is similar to the low reported incidence of 2.4% in Abouzeid's study. In contrast, the incidence was reported to be as high as 17.1% in the series by Schueler et al in which a higher dose was employed. Proliferative retinopathy has been reported to occur in 13%-19% after ^{125}I plaque brachytherapy in which dose reached further than ^{106}Ru.

$BED_3 \geqq 1200$ Gy_3 of the outer surface of sclera was significantly correlated with the incidence of either retinal detachment or proliferative retinopathy or rubeosis (Fig. 3b). A higher dose for sclera was demonstrated to cause late complications associated with RPT; therefore, it is important to exclude tall tumors whose dose of the outer surface of sclera will be high in order to avoid complications. However, there were only 2 enucleations caused by the late complications of RPT, and RPTs were generally well tolerated.

There were 2 secondary malignancies in the current series. Both of them occurred in the patients with a hereditary retinoblastoma, 1 of them developed within the EBRT fields. In accordance with the literature (6, 7), plaque brachytherapy itself did not seem to increase the incidence of secondary malignancy.

Conclusion

RPT is an effective and safe focal therapy for retinoblastoma. However, optimal dose of RPT remains to be studied further.

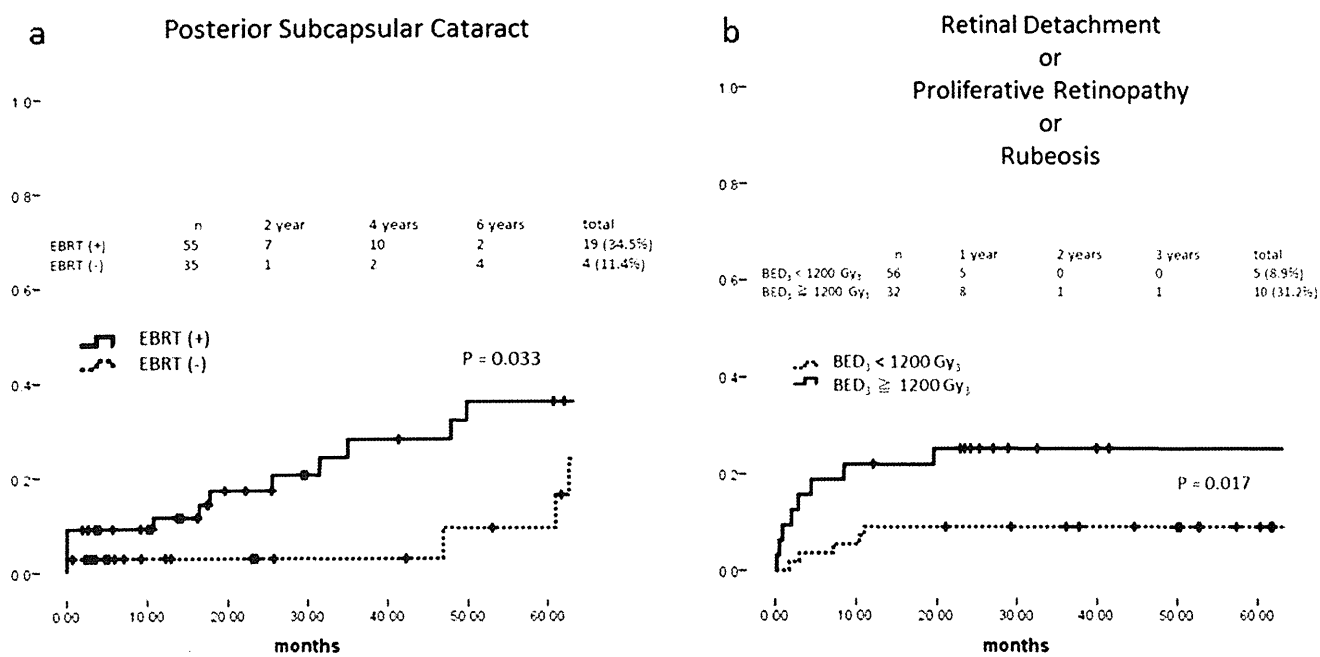

Fig. 3. (a) Cumulative incidence of posterior subcapsular cataract according to whether external beam radiation therapy (EBRT) was administered. (b) Cumulative incidence of retinal detachment, proliferative retinopathy and rubeosis stratified by biological effective dose (BED) with $\alpha/\beta = 3$ Gy at the outer surface of sclera.

References

1. National registry of retinoblastoma in Japan (1975–1982). The Committee for the National Registry of Retinoblastoma. *Nippon Ganka Gakkai Zasshi* 1992;96:1433-1442.
2. Kleinerman RA, Tucker MA, Tarone RE, et al. Risk of new cancers after radiotherapy in long-term survivors of retinoblastoma: an extended follow-up. *J Clin Oncol* 2005;23:2272-2279.
3. Abramson DH, Schefler AC. Update on retinoblastoma. *Retina* 2004; 24:828-848.
4. Lin P, O'Brien JM. Frontiers in the management of retinoblastoma. *Am J Ophthalmol* 2009;148:192-198.
5. Freire JE, De Potter P, Brady LW, et al. Brachytherapy in primary ocular tumors. *Semin Surg Oncol* 1997;13:167-176.
6. Shields CL, Shields JA, Cater J, et al. Plaque radiotherapy for retinoblastoma: long-term tumor control and treatment complications in 208 tumors. *Ophthalmology* 2001;108:2116-2121.
7. Shields CL, Mashayekhi A, Sun H, et al. Iodine 125 plaque radiotherapy as salvage treatment for retinoblastoma recurrence after chemoreduction in 84 tumors. *Ophthalmology* 2006;113:2087-2092.
8. Schueler AO, Fluhs D, Anastassiou G, et al. Beta-ray brachytherapy with 106Ru plaques for retinoblastoma. *Int J Radiat Oncol Biol Phys* 2006;65:1212-1221.
9. Abouzeid H, Moeckli R, Gaillard MC, et al. (106)Ruthenium brachytherapy for retinoblastoma. *Int J Radiat Oncol Biol Phys* 2008;71: 821-828.
10. Nag S, Quivey JM, Earle JD, et al. The American Brachytherapy Society recommendations for brachytherapy of uveal melanomas. *Int J Radiat Oncol Biol Phys* 2003;56:544-555.
11. Jarvien H, Cross WG, Soares C, et al. Dosimetry of beta rays and low-energy photons for brachytherapy with sealed sources. *J ICRU* 2004;4: 2-175.
12. Linn Murphree A. Intraocular retinoblastoma: the case for a new group classification. *Ophthalmol Clin North Am* 2005;18:41-53. viii.
13. Shields CL, Mashayekhi A, Au AK, et al. The International Classification of Retinoblastoma predicts chemoreduction success. *Ophthalmology* 2006;113:2276-2280.
14. BEBIG. BEBIG Ruthenium Augenapplikatoren Kundeninformation: Einführung der neuen NIST-kalibrierten Dosimetrie Einführung der neuen PTB-kalibrierten Aktivitätsmessungen. 2002:version 1.03 v. 12.11.02.
15. Dale RG. The application of the linear-quadratic dose-effect equation to fractionated and protracted radiotherapy. *Br J Radiol* 1985;58:515-528.
16. Kaplan EL, Meier P. Nonparametric estimation from incomplete observations. *J Am Stat Assoc* 1958;53:457-481.
17. Yamane T, Kaneko A, Mohri M. The technique of ophthalmic arterial infusion therapy for patients with intraocular retinoblastoma. *Int J Clin Oncol* 2004;9:69-73.
18. Oosterhuis JA, Journee-de Korver HG, Kakebeeke-Kemme HM, et al. Transpupillary thermotherapy in choroidal melanomas. *Arch Ophthalmol* 1995;113:315-321.
19. Foote RL, Garretson BR, Schomberg PJ, et al. External beam irradiation for retinoblastoma: patterns of failure and dose-response analysis. *Int J Radiat Oncol Biol Phys* 1989;16:823-830.
20. Hernandez JC, Brady LW, Shields JA, et al. External beam radiation for retinoblastoma: results, patterns of failure, and a proposal for treatment guidelines. *Int J Radiat Oncol Biol Phys* 1996;35: 125-132.

J Cancer Res Clin Oncol (2012) 138:1239–1247
DOI 10.1007/s00432-012-1198-y

ORIGINAL PAPER

Effect of chemotherapy on survival after whole brain radiation therapy for brain metastases: a single-center retrospective analysis

Hiroshi Mayahara · Minako Sumi · Yoshinori Ito · Syuhei Sekii · Kana Takahashi · Kouji Inaba · Yuuki Kuroda · Naoya Murakami · Madoka Morota · Jun Itami

Received: 10 January 2012 / Accepted: 5 March 2012 / Published online: 23 March 2012

Abstract
Background and purpose Whether chemotherapy for systemic disease affects survival of patients with brain metastases or not has not been elucidated before. We performed comprehensive analysis of patients with newly-diagnosed brain metastases primarily treated with whole brain radiation therapy (WBRT) alone.
Materials and methods Data from 134 patients with newly-diagnosed brain metastases primarily treated with WBRT from 2007 to 2008 was retrospectively reviewed. Univariate and multivariate analyses were performed to identify significant prognostic factors.
Results Median survival time (MST) of this cohort from the start of WBRT was 5.7 months. MST of patients with RPA Class 1, 2 and 3 were 10.3, 7.8 and 2.2 months, respectively. Multivariate analysis revealed that karnofsky performance status ($\geq$70, $p < 0.0001$), gender (female, $p < 0.0001$), activity of extracranial disease (stable, $p = 0.015$), time to develop brain metastasis (<3 months, $p = 0.042$) and use of chemotherapy after WBRT (multiple regimens, $p < 0.0001$) were independent prognostic factors for better survival.
Conclusions Systemic chemotherapy for chemo-responsive cancer prolongs survival despite the presence of treated brain metastases. Irradiated brain metastases will lose their prognostic significance in a large number of patients. Systemic chemotherapy will be a treatment of choice for patients who have systemic disease after WBRT for brain metastases. These results should be validated in the future prospective clinical trials.

Keywords Brain metastasis · Brain metastases · Radiation therapy · Whole brain radiation therapy · Chemotherapy · Prognostic factors

Introduction

Brain metastasis affects 20–40 % of cancer patients (Soffietti et al. 2002). Brain metastasis is one of the major causes of morbidity in cancer patients. The prognosis of patients with brain metastasis is generally poor with a median survival time (MST) of 1–2 months with corticosteroids only (Weissman 1988; Lagerwaard et al. 1999).

The route of metastatic dissemination to the brain is often hematogeneous, therefore, the entire brain can be seeded with micrometastatic focus. Traditionally, whole brain radiation therapy (WBRT) has been regarded as the standard treatment for patients with brain metastasis. Overall survival of the patients after WBRT ranges 3–6 months (Lagerwaard et al. 1999; Gaspar et al. 2010; Tsao et al. 2005). Various dose/fractionation schedules of WBRT were tested in clinical studies, which resulted in no significant difference in median survival time after WBRT (Tsao et al. 2005; Gaspar et al. 2010).

Recently, significant progress has been made for a subset of patients with single or few brain metastases and well controlled systemic disease. Surgical resection or stereotactic radiosurgery (SRS) combined with WBRT significantly prolonged survival (Patchell et al. 1990; Vecht et al. 1993; Andrews et al. 2004). Median survival of

This study was presented in part at the 53rd Annual Meeting of the American Society for Radiation Oncology in Miami, October 2-6, 2011.

H. Mayahara (✉) · M. Sumi · Y. Ito · S. Sekii · K. Takahashi · K. Inaba · Y. Kuroda · N. Murakami · M. Morota · J. Itami
Division of Radiation Oncology, National Cancer Center Hospital, 5-1-1 Tsukiji, Chuo-ku, Tokyo 104-0045, Japan
e-mail: hmayahar@ncc.go.jp

patients who received these aggressive therapies ranges 7–10 months. Unfortunately, patients who entered into these clinical trials represent only a small minority of the patients with brain metastases. For the majority of patients with multiple brain metastases and uncontrolled systemic disease, only WBRT is the standard treatment of choice.

The role of chemotherapy in brain metastasis has been limited because of the concern about the activity of chemotherapeutic agent to cross the blood–brain barrier (BBB). Recently, the activity of chemotherapy in brain metastasis is highlighted (Robinet et al. 2001; Walbert and Gilbert 2009; Mehta et al. 2010). Concurrent chemoradiation therapies with BBB permeable agents, such as Temozolamide or topotecan are currently under investigation in prospective clinical trials. Some investigators suggested that the permeability of BBB can alter after fractionated radiotherapy for brain metastasis (Yuan et al. 2006; Wilson et al. 2009). However, whether the use of chemotherapy affects survival of the patients with brain metastasis or not has not been elucidated before.

The primary aim of this study was to perform comprehensive analysis of 134 consecutive patients with newly-diagnosed brain metastases primarily treated by WBRT alone in a single institution. The secondary aim was to define independent prognostic factors associated with longer survival after WBRT. The final aim was to investigate the prognostic value of chemotherapy on survival after WBRT in patients with brain metastases.

Materials and methods

Patient characteristics

The database of patients who underwent radiotherapy for brain metastases at our institution was reviewed. A total of 264 patients were treated with WBRT between 2007 and 2008. Of these, 23 patients received WBRT as a salvage therapy after SRS. Another 39 patients received WBRT as an adjuvant therapy after resection of metastatic brain tumor. Forty-seven patients were metastases from radiosensitive primary tumor such as leukemia, lymphoma or small cell carcinoma. Excluding these patients, we reviewed the medical records of 155 patients with newly diagnosed brain metastases treated with WBRT as a primary therapy. Of these, 19 patients presented with symptoms or radiographic findings of leptomeningeal metastasis. We excluded these patients with leptomeningeal metastasis because they are known to have extremely limited survival. Two patients were ineligible for evaluation because of allergy to contrast media. Finally, a group of 134 patients were subjected to extensive analysis. The clinical and image interpretation data from these patients were entered into database in December 2010. Distribution of baseline patient and tumor characteristics is shown in Table 1.

Table 1 Distribution of baseline patient and tumor characteristics

Parameters	*n*	%	Parameters	*n*	%
Median age (years)	60		Extracranial distant metastases		
Gender			Absent	11	8
Male	69	51	Stable	16	12
Female	65	49	Progressive	107	80
Karnofsky performance status (KPS)			Activity of extracranical tumor		
100–90	46	34	Absent/stable	20	15
80–70	49	37	Progressive	114	85
60–50	29	22	Time to diagnosis of brain metastasis		
40–0	10	7	<3 months	21	16
Neurologic status			3–12 months	33	25
0	45	34	1–2 years	22	16
1	27	20	≥2 years	58	43
2	34	25	Type of the diagnostic brain image		
3	21	16	MRI	106	79
4	7	5	CT	28	21
RPA criteria			Number of brain metastases		
Class 1	5	4	1–4	40	30
Class 2	91	68	5–10	39	29
Class 3	38	28	11–24	29	22
Site of primary tumor			≥25	26	19
Lung	75	56	Size of the largest lesion		
Breast	27	20	≤10	31	23
Upper gastrointestinal tract	11	8	11–20	46	34
Colorectum	10	8	21–30	34	25
Genitourinary tract	5	4	>30	23	17
Others	6	5	Chemotherapeutic regimens before WBRT		
Histological type			None	22	16
Adenocarcinoma	114	85	Single	28	21
Squamous cell carcinoma	9	7	Multiple	84	63
Others	11	8	Chemotherapeutic regimens after WBRT		
Primary tumor status			None	70	52
Absent	57	42	Single	31	23
Stable	25	19	Multiple	33	25
Progressive	52	39	Molecular targeted therapy after WBRT (>1 month)		
			No	100	74
			Yes	34	26

RPA recursive partitioning analysis, *MRI* magnetic resonance imaging, *CT* computed tomography, *WBRT* whole brain radiation therapy

Imaging studies

Diagnosis of brain metastases was performed mainly with magnetic resonance images (MRI). In our institute, all patients with lung cancer routinely undergo brain imaging for initial staging or scheduled follow-up. Patients with other solid tumors underwent brain imaging when brain metastasis is clinically suspected. In this study, initial diagnostic brain images included MRI in 106 patients (79 %) and CT in 28 patients (21 %). Radiological features assessed included number, maximum tumor diameter and location. For follow-up brain images, change in size of the tumors and presence of new metastases were recorded. At least 20 % increase in diameter of the each preexisted tumor before WBRT, taking as reference on the smallest diameter after WBRT, was defined as local progression.

Treatment strategy

Treatment strategy for brain metastasis at our institution was previously described elsewhere (Narita and Shibui 2009; Hashimoto et al. 2011). Patients who received WBRT alone as a primary treatment for brain metastases were subjected for this study. Patients with brain metastases generally have extracranial systemic disease. After WBRT, patients with known systemic disease were indicated to start or continue chemotherapy if they still had active chemotherapeutic regimen with sufficient organ function and with Karnofsky performance status (KPS) of 70 or more. Salvage SRS was considered for recurrent brain metastases after WBRT. Some patients with known chemo-sensitive tumor continued palliative chemotherapy for recurrent brain metastases.

Consent for the treatment was obtained from each patient after the sufficient explanation of potential risks of treatment. All the patients provided written informed consent. Our institutional review board has approved this study.

Whole brain radiation therapy

One hundred and thirty-four patients were intended to receive WBRT. Of these, 128 patients were delivered to a dose of 30 Gy in 10 fractions. Another 3 patients were delivered to 37.5 Gy in 15 fractions, whereas one patient was delivered to 20 Gy in 5 fractions. Two patients discontinued irradiation course because of the deterioration of general condition at a dose of 12 and 24 Gy, respectively.

Retrospective analysis

All the medical charts of the eligible patients were reviewed. Information on potential prognostic factors (age, gender, KPS, neurologic status, site of primary tumor, primary tumor status, activity of extracranial distant metastases, time to develop brain metastasis, number of brain metastases, size of the largest lesion, use of chemotherapy before or after WBRT) was collected.

Initial neurological function was classified into 4 categories (No symptoms: grade 0, Minor symptoms; fully active without assistance: grade 1, Moderate symptoms; fully active but requires assistance: grade 2, Moderate symptoms; less than fully active: grade 3, Severe symptoms; totally inactive: grade 4). Radiation Therapy Oncology Group's (RTOG) recursive partitioning analysis (RPA) classes were coded into 3 categories as follows: Class 1: Patients with KPS $\geq$ 70, <65 years of age with controlled primary and no extracranial metastases; Class 3: KPS $<$ 70; Class 2: all the others (Gaspar et al. 1997).

For the evaluation of extracranial disease status, if there were no evidence of residual tumor after therapy, the activity was coded as "absent". If any tumor existed and there is no increase in size of the tumor for more than 6 months, the activity was coded as "stable". A continuous use of same chemotherapeutic regimen didn't impair the coding of "stable". If any tumor existed with any situation other than "stable", the activity was coded as "progressive".

Patients whose brain metastases were detected at the same time or soon after the diagnosis of primary tumor (so-called "synchronous" brain metastasis) may have different prognosis. We defined "synchronous" brain metastasis as those detected at the same time or detected within 3 months of the initial diagnosis of primary tumor.

For the analysis of prognostic effect of chemotherapy before or after WBRT, three different cohorts were defined: none, single regimen and multiple regimens. If a patient received two or more different types of chemotherapeutic regimens, the status was coded as multiple regimens. Any type of hormonal therapy was regarded as a single regimen. The status of the use of molecular targeted therapy was defined as "yes", if a patient continued to receive a specific regimen for more than 1 month.

Statistical analysis

Overall survival from the start of WBRT was calculated with the Kaplan–Meier method. For univariate and multivariate analysis, all the variables were dichotomized according to the clinical relevance from previous literature. Univariate analyses were performed by using log-rank test. Possible confounded variables were excluded from multivariate analysis. A Cox's proportional hazards model was developed to identify significant factors influencing survival after WBRT. All the tests of hypotheses were

conducted at the alpha level of 0.05 with a 95 % confidence interval. All the statistical analyses were performed by using SPSS Statistics version 17.0 (SAS Institute, Tokyo, Japan).

Results

Outcomes for the entire group

Median survival time (MST) for the entire patients from the start of WBRT was 5.7 months. The 6 months, 1- and 2-year survival rate were 43, 28 and 12 %, respectively. MST of the patients with RTOG's RPA Class 1 ($n = 5$), 2 ($n = 91$) and 3 ($n = 38$) were 10.3, 7.8 and 2.2 months, respectively (Fig. 1). Median intracranial progression-free survival (PFS) were 4.7 months, with 6 months, 1- and 2-year PFS of 35, 14 and 4 %, respectively. A total of 49 patients developed intracranial recurrence after WBRT. The sites of first recurrence after WBRT were as follows: local only (regrowth of preexisted tumors): 25 (51 %); new metastasis only: 10 (20 %); both of local and new metastasis: 12 (24 %); and leptomeningeal dissemination: 2 (4 %). Median local progression-free duration and median intracranial new metastasis-free duration for the entire patients were 9.7 and 18.0 months, respectively. At the time of analysis, 5 patients were alive with disease. The causes of death were identified in 118 patients. Of these, 38 patients (32 %) were due to intracranial tumor progression, whereas 76 patients (64 %) were due to systemic disease. Four patients (3 %) died from intercurrent disease. None had died directly from toxicity of WBRT.

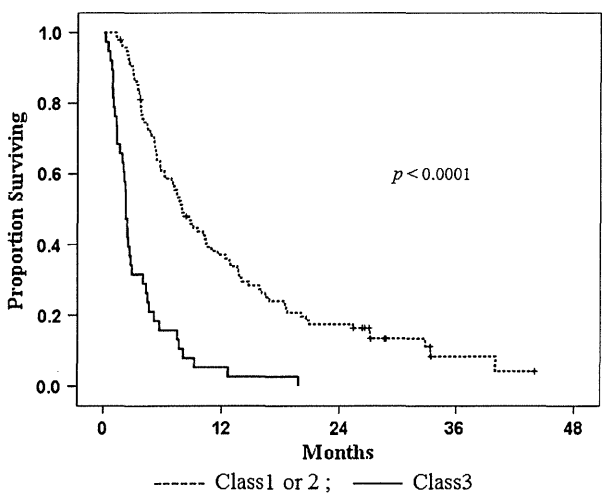

Fig. 1 Kaplan–Meier survival curve for overall survival by RPA criteria

Factors influencing survival after WBRT: univariate and multivariate analyses

Univariate analysis was performed on 12 different variables to evaluate their potential value on survival after WBRT. Univariate analyses identified 9 variables which significantly associated with good prognosis (Table 2).

Multivariate analysis was performed on 9 independent variables. Table 3 summarizes the result of the multivariate analysis for survival after WBRT. Multivariate analysis revealed that KPS ($\geq$70 vs. 70, hazard rate (HR): 2.540, $p < 0.0001$), gender (female vs. male, HR: 2.293, $p < 0.0001$), activity of extracranial disease (absent/stable vs. progressive, HR: 2.134, $p = 0.015$), time to develop brain metastasis (<3 vs. $\geq$3 months, HR: 1.926, $p = 0.042$), and use of chemotherapy after WBRT (multiple vs. none/single regimens, HR: 3.406, $p < 0.0001$) were independent prognostic factors for overall survival.

Survivals depending on chemotherapy after WBRT

After WBRT, only two patients had no evidence of extracranial tumor. The two patients didn't receive further chemotherapy until disease progression. Another 132 patient had known extracranial tumor including primary, nodal or distant sites. They were indicated to start or continue chemotherapy when it was clinically applicable. A total of 64 patients with extracranial systemic disease underwent chemotherapy after WBRT. Thirty-one patients (23 %) received only a single chemotherapeutic regime, and 33 patients (25 %) received multiple regimens. Figure 2 shows the survival curve by the use of chemotherapy after WBRT. The MST of the patients who received none, single and multiple regimens after WBRT were 3.3, 7.5 and 16.4 months, respectively ($p < 0.0001$). The use of multiple chemotherapeutic regimens after WBRT was found to be associated with better survival after WBRT in multivariate analysis ($p < 0.0001$). Among 95 patients with pre-irradiation KPS $\geq$ 70, 59 patients (62 %) received chemotherapy, whereas 5 patients (13 %) with KPS < 70 received chemotherapy. Among patients with KPS $\geq$ 70, the MST of the patients who received none, single and multiple regimens after WBRT were 4.5, 7.9 and 16.4 months, respectively ($p < 0.0001$). Overall, 95 % of the patients included in this study received chemotherapy either before or after WBRT.

The effect of molecular-targeted therapy after WBRT

A total of 34 patients (25 %) received molecular-targeted therapy after WBRT for 1 month or more. Of these patients, the sites of primary disease were lung in 28, breast

Table 2 Results of univariate analyses for survival after WBRT

Parameters	*n*	Median survival time (months)	6-months survival (%)	1-year survival (%)	2-year survival (%)	*p* value
Overall patients	134	5.7	43	28	12	–
Age						
<65	87	7.4	54	31	13	
≥65	47	4.9	38	22	11	0.31
Gender						
Male	69	4.5	32	17	6	
Female	65	9.1	66	40	20	0.0009
Karnofsky performance status						
≥70	95	7.9	62	39	17	
<70	39	2.2	15	3	0	<0.0001
Neurologic status						
0–1	72	7.9	58	44	22	
2–4	62	4.5	36	1	0	<0.0001
RPA criteria						
Class 1–2	96	7.9	61	37	18	
Class 3	38	2.2	16	5	0	<0.0001
Site of primary tumor						
Lung	75	7.4	55	39	21	
Others	59	4.5	39	14	2	0.001
Activity of extracranical tumor						
Absent/stable	20	9.1	60	40	25	
Progressive	114	5.2	46	26	10	0.015
Time to develop brain metastasis						
<3 months	21	16.9	75	65	40	
≥3 months	113	5.2	43	21	7	0.002
Number of brain metastasis						
1–4	40	5.1	39	21	10	
≥5	94	6.2	52	31	13	0.53
Size of the largest lesion						
<20 mm	69	7.4	53	36	16	
≥20 mm	65	5.1	42	20	8	0.11
Chemotherapeutic regimens before WBRT						
None/single	50	7.2	52	42	20	
Multiple	84	5.2	46	19	8	0.019
Chemotherapeutic regimens after WBRT						
None/single	101	4.0	33	13	4	
Multiple	33	16.4	94	73	36	<0.0001

RPA recursive partitioning analysis, *WBRT* whole brain radiotherapy

in 5 and kidney in 1. All of the histological diagnoses of lung primary patients were adenocarcinoma. Twenty-seven lung primary patients received epidermal growth factor receptor-tyrosine kinase inhibitor (EGFR-TKI) for a median duration of 7 months. Figure 3 shows the survival curve by the use of molecular-targeted therapy after

Table 3 Results of multivariate analysis for survival after WBRT

Variables	Factors	Hazard rate (95 % CI)	*p* value
Karnofsky performance status	≥70 versus <70	2.540 (1.627–3.966)	<0.0001
Gender	Female versus male	2.293 (1.541–3.412)	<0.0001
Extracranial disease status	Absent/stable versus progressive	2.134 (1.160–3.928)	0.015
Time to develop brain metastasis	<3 versus ≥3 months	1.926 (1.025–3.620)	0.042
Number of chemotherapeutic regimens after WBRT	Multiple regimens versus none/single regimen	3.406 (2.013–5.761)	<0.0001

CI confidence interval, *WBRT* whole brain radiation therapy

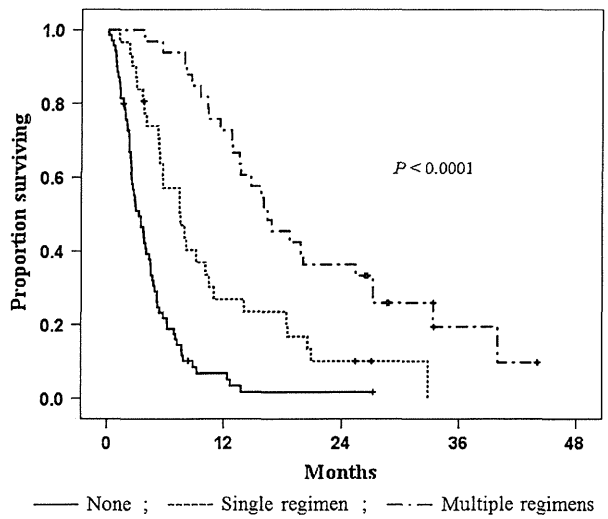

Fig. 2 Kaplan–Meier overall survival curve by the use of chemotherapeutic regimen after WBRT

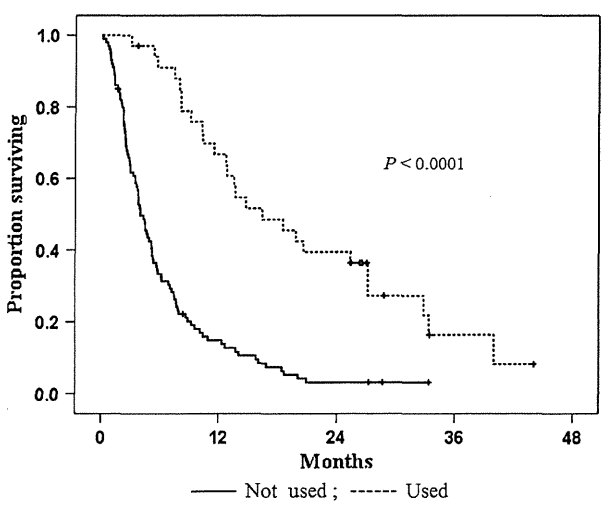

Fig. 3 Kaplan–Meier overall survival curve by the use of molecular-targeted therapy after WBRT

WBRT. The MST of the patients who received molecular-targeted therapy after WBRT was significantly longer than that of those who did not (16.4 vs. 4.0 months, $p < 0.0001$).

Discussion

Significant progress has been made over the last decades for a subset of patients with single or few brain metastases and well controlled systemic disease. In prospective randomized clinical trials, surgical resection or SRS combined with WBRT significantly prolonged survival in selected patients with single or few brain metastases (Patchell et al. 1990; Vecht et al. 1993; Andrews et al. 2004). MST of these patients who received combined therapy ranges 7–10 months. SRS alone in patients with one or few brain metastases was comparable to SRS combined with WBRT at least in terms of overall survival, with a MST of 8 months (Aoyama et al. 2006). Unfortunately, the patients who entered into these clinical trials represent only a small minority of patients with brain metastases. In clinical practice, it remains unclear whether these aggressive therapies have sufficient benefit for the majority of patients with uncontrolled systemic disease or numerous brain metastases. Currently, only WBRT is the standard treatment of choice for these patients. The indication of SRS for patients with brain metastases in clinical practice continues to be a matter of debate.

Various prospective and retrospective studies have shown that the treatment modality is the first most important prognostic factor on long-term survival, although the effect of patient selection bias is inevitable (Andrews et al. 2004; Lagerwaard et al. 1999; Patchell et al. 1990). To minimize the selection bias, we investigated only patients primarily treated with WBRT alone in this study. Numerous studies on prognostic factors in patients with brain metastases have been published previously. The results of this study re-confirmed the value of established prognostic factors reported in the literature. Multivariate analysis showed that good KPS, stable extracranial disease and female gender were independent predictors of better survival after WBRT, in line with previous literatures (Lagerwaard et al. 1999; Patchell et al. 1990; Aoyama et al. 2006; Gaspar et al. 1997; Swinson and William 2008). Dose these pretreatment characteristics fully determine the prognosis of patients with brain metastases?

Performance status is regarded as the second most important prognostic factor in patient's characteristics (Lagerwaard et al. 1999; Aoyama et al. 2006; Gaspar et al. 1997; Fleckenstein et al. 2004; 20). Generally, patients with low KPS are not indicated for aggressive therapy other than WBRT alone. In this study, the MST of the patients with KPS < 70 was only 2.2 months. The Performance status of the patients with brain metastases frequently deteriorated by extended intracranial disease. Additionally, patients with very low performance status were not indicated for further chemotherapy despite the existence of systemic disease. In this study, only 5 patients (13 %) with pre-treatment KPS < 70 received chemotherapy after WBRT. We conclude that poor survival time of the patients with low KPS is due to the systematic disease progression, as well as intracranial disease progression.

In line with our study, activity of extracranial primary disease is the third most important prognostic factor reported in the literature (Lagerwaard et al. 1999; Aoyama et al. 2006; Fleckenstein et al. 2004; 20). These finding suggests that survival of patients with brain metastases is in a large part, regulated by the extracranial status. Seventy-six patients (64 %) included in this study died due to systemic disease. This percentage is comparable to the reports of prospective clinical trials with SRS alone or SRS + WBRT for single or fewer numbers of brain metastases with well controlled systemic disease (Sneed et al. 1999; Andrews et al. 2004; Aoyama et al. 2006). This result highlights the modest effectiveness of WBRT on brain metastases. WBRT alone have adequate efficacy to avoid neurologic death for about two-thirds of patients with brain metastases. If we consider the high morbidity rate from systemic disease after WBRT, chemotherapy is the primary therapeutic approach for the control of extracranial disease. Therefore, systemic chemotherapy for chemo-responsive cancer prolongs survival despite the presence of treated brain metastases. Irradiated brain metastases will lose their prognostic significance in a large number of patients.

The role of chemotherapy in brain metastasis itself has been limited. Although there is some breakdown of blood–brain barrier (BBB) around brain metastases, the concentrations of most of the chemotherapeutic agents are still very limited within the lesion (Gerstner and Fine 2007). However, some chemotherapeutic agents are known to have activity of crossing BBB. Temozolomide (TMZ) is a third generation alkylating agent, and it can cross the BBB because of its small size and lipophilic properties (Ostermann et al. 2004). Some clinical trials suggest that single agent TMZ has some activity in patients with recurrent brain metastases (Christodoulou et al. 2001; Siena et al. 2010). Several Phase II clinical trials of TMZ combined with WBRT were performed with promising results (Antonadou et al. 2002; Addeo et al. 2008). These trials proved improved response rate and neurologic function with addition of TMZ to WBRT. A phase III clinical trial of WBRT plus SRS with or without TMZ or Erlotinib in patients with brain metastases is now ongoing (ClinicalTrials.gov identifier: NCT00096265). Patients with 1–3 brain metastases from histologically confirmed non-small cell lung cancer, well circumscribed, maximum diameter of 4 cm or less, no metastasis within 10 mm of the optic apparatus, no metastasis in the brain stem and stable extracranial metastases are enrolled. Patients are randomized to three groups: Arm 1: WBRT + SRS, Arm 2: WBRT + SRS + TMZ, Arm 3: WBRT + SRS + erlotinib. Patients in Arm 2 and 3 begin TMZ or erlotinib on the first day of WBRT and continue up to 6 months. The primary endpoint is overall survival, and secondary endpoint includes time to CNS progression, performance status at 6 months, steroid dependence at 6 months, cause of death and effect of non-protocol chemotherapy.

Topotecan is a semi-synthetic analogue of the alkaloid camptothecin, which selectively inhibits topoisomerase I. Topotecan crosses the BBB, because of its low protein binding property (Baker et al. 1996). Single agent topotecan has positive activity in patients with brain metastases from small cell lung cancer (Korfel et al. 2002). A phase III multicentric clinical trial of topotecan and WBRT for patients with brain metastases form lung cancer was planned, however, was terminated because of low patient accrual (Neuhaus et al. 2009). This trial failed to show clear benefit of adding topotecan to WBRT. Another multicentric phase III clinical trial is ongoing (ClinicalTrials.gov identifier: NCT00390806). Patients with at least one brain metastasis form non-small cell lung cancer, who have received previous chemotherapy are enrolled. Patients are randomized to two groups: experimental arm: topotecan + WBRT, control arm: WBRT alone. The primary endpoint is overall survival, secondary endpoint includes response rate, time to response, time to progression, brain tumor symptom, safety and tolerability. We think that these clinical trials for brain metastasis should evaluate the effect of non-protocol chemotherapy on survival. In the next 5 years, the results of these phase III, multicentric clinical trials will become available to further define the role of these chemotherapeutic agents when combined with WBRT and SRS, or both.

Some investigators suggest that the permeability of BBB in brain tumors can alter during or ever after fractionated radiotherapy (Yuan et al. 2006; Wilson et al. 2009; Cao et al. 2005). After irradiation, the BBB may be partially disrupted so that some chemotherapeutic agents can reach a therapeutic level in the metastatic tumors. This is another explanation of the value of systemic chemotherapy after WBRT. In fact, subset analysis of this study showed that

the use of chemotherapy after WBRT was also an independent prognostic factor predicting longer local tumor progression-free duration (data not shown). We believe that some brain metastases become sensitive to chemotherapy after irradiation. Chemo-sensitivity of brain metastases can affect the survival of a part of patients with treated brain metastases. Therefore, systemic chemotherapy will be a treatment of choice for those who have systemic disease with irradiated brain metastases. If a patient have a plan of definitive chemotherapy for primary disease after the treatment of brain metastases, such patient can be a good candidate for more aggressive therapy for brain metastases.

Another topic of debate is whether molecular-targeted therapy has a significant role on brain metastasis or not. Some investigators advocated that EGFR-TKI has promising activity on previously untreated brain metastases from lung adenocarcinoma (Wu et al. 2007; Kim et al. 2009; Katayama et al. 2009). Another investigator reported activity of trastuzumab on brain metastasis from HER2-overexpressing breast cancer (Park et al. 2009). In this study, the MST of the patients who received molecular-targeted therapy after WBRT was significantly longer than that of those who did not. In the subset analysis of this study, use of molecular-targeted therapy after WBRT was also a significant predictor of longer local progression-free duration (data not shown). We believe that molecular-targeted therapy could have some activity on the local control of some brain metastases.

Patients with "synchronous" brain metastasis survived significantly longer than "metachronous" brain metastasis patients in this study. Short time to develop brain metastasis was marginally independent prognostic factor in multivariate analysis. This is in line with a literature of surgical removal or SRS for brain metastasis (Flannery et al. 2008; Bonnette et al. 2001; Hu et al. 2006). It is easy to assume that systematic disease of patients with "synchronous" brain metastasis would more likely to respond to the following chemotherapy. The "synchronous" brain metastasis may be more sensitive to radiotherapy, when compared to brain metastasis emerged after repeated chemotherapies. Also in agreement with some literature (Lagerwaard et al. 1999; Swinson and William 2008), female patients survived significantly longer than male patients. In particular, the prognosis of female patients with brain metastasis form lung primary has reported to be significantly better than that of male patients (Lagerwaard et al. 1999; Sánchez de Cos et al. 2009). We should further continue to investigate these clinical characteristics of brain metastases.

We acknowledge that the present study had certain limitations because of its retrospective nature. First, the results of this study might be highly influenced by patient's selection bias. Patients with brain metastases which well responded to WBRT may have more opportunity for receiving multiple chemotherapy after WBRT. Second, our cohort should deviate to patients with numerous brain metastases with uncontrolled systemic disease. Because we included only patients with brain metastases primarily treated by WBRT alone, patients with poor prognosis should be negatively selected for this study. Currently, we are investigating the patients with one or few brain metastases primarily treated by SRS alone, and it will be described in another report. Actual prognostic value of chemotherapy on survival after WBRT for brain metastases should be validated in future prospective clinical trials.

Conclusions

In addition to the confirmed prognostic factors previously reported in the literature, the use of multiple chemotherapeutic regimens after WBRT was associated with better survival. Systemic chemotherapy for chemo-responsive cancer prolongs survival despite the presence of treated brain metastases. Irradiated brain metastases will lose their prognostic significance in a large number of patients. Systemic chemotherapy will be a treatment of choice for patients who have systemic disease after WBRT for brain metastases. These results should be validated in future prospective clinical trials.

Conflict of interest None.

References

Addeo R, De Rosa C, Faiola V et al (2008) Phase 2 trial of temozolomide using protracted low-dose and whole-brain radiotherapy for nonsmall cell lung cancer and breast cancer patients with brain metastases. Cancer 113:2524–2531

Andrews DW, Scott CB, Sperduto PW et al (2004) Whole brain radiation therapy with or without stereotactic radiosurgery boost for patients with one to three brain metastases: phase III results of the RTOG 9508 randomised trial. Lancet 363:1665–1672

Antonadou D, Paraskevaidis M, Sarris G et al (2002) Phase II randomized trial of temozolomide and concurrent radiotherapy in patients with brain metastases. J Clin Oncol 20:3644–3650

Aoyama H, Shirato H, Tago M et al (2006) Stereotactic radiosurgery plus whole-brain radiation therapy vs. stereotactic radiosurgery alone for treatment of brain metastases: a randomized controlled trial. JAMA 295:2483–2491

Baker SD, Heideman RL, Crom WR et al (1996) Cerebrospinal fluid pharmacokinetics and penetration of continuous infusion topotecan in children with central nervous system tumors. Cancer Chemother Pharmacol 37:195–202

Bonnette P, Puyo P, Gabriel C et al (2001) Surgical management of non-small cell lung cancer with synchronous brain metastases. Chest 119:1469–1475

Cao Y, Tsien CI, Shen Z et al (2005) Use of magnetic resonance imaging to assess blood-brain/blood-glioma barrier opening during conformal radiotherapy. J Clin Oncol 23:4127–4136

Christodoulou C, Bafaloukos D, Kosmidis P et al (2001) Phase II study of temozolomide in heavily pretreated cancer patients with brain metastases. Ann Oncol 12:249–254

Flannery TW, Suntharalingam M, Regine WF et al (2008) Long-term survival in patients with synchronous, solitary brain metastasis from non-small-cell lung cancer treated with radiosurgery. Int J Radiat Oncol Biol Phys 72:19–23

Fleckenstein K, Hof H, Lohr F et al (2004) Prognostic factors for brain metastases after whole brain radiotherapy. Strahlenther Onkol 180:268–273

Gaspar L, Scott C, Rotman M et al (1997) Recursive partitioning analysis (RPA) of prognostic factors in three Radiation Therapy Oncology Group (RTOG) brain metastases trials. Int J Radiat Oncol Biol Phys 37:745–751

Gaspar LE, Mehta MP, Patchell RA et al (2010) The role of whole brain radiation therapy in the management of newly diagnosed brain metastases: a systematic review and evidence-based clinical practice guideline. J Neurooncol 96:17–32

Gerstner ER, Fine RL (2007) Increased permeability of the blood-brain barrier to chemotherapy in metastatic brain tumors: establishing a treatment paradigm. J Clin Oncol 25:2306–2312

Hashimoto K, Narita Y, Miyakita Y et al (2011) Comparison of clinical outcomes of surgery followed by local brain radiotherapy and surgery followed by whole brain radiotherapy in patients with single brain metastasis: single-center retrospective analysis. Int J Radiat Oncol Biol Phys 81:e475–e480

Hu C, Chang EL, Hassenbusch SJ III et al (2006) Nonsmall cell lung cancer presenting with synchronous solitary brain metastasis. Cancer 106:1998–2004

Katayama T, Shimizu J, Suda K et al (2009) Efficacy of erlotinib for brain and leptomeningeal metastases in patients with lung adenocarcinoma who showed initial good response to gefitinib. J Thorac Oncol 4:1415–1419

Kim JE, Lee DH, Choi Y et al (2009) Epidermal growth factor receptor tyrosine kinase inhibitors as a first-line therapy for never-smokers with adenocarcinoma of the lung having asymptomatic synchronous brain metastasis. Lung Cancer 65:351–354

Korfel A, Oehm C, von Pawel J et al (2002) Response to topotecan of symptomatic brain metastases of small-cell lung cancer also after whole-brain irradiation. A multicentre phase II study. Eur J Cancer 38:1724–1729

Lagerwaard FJ, Levendag PC, Nowak P et al (1999) Identification of prognostic factors in patients with brain metastases: a review of 1292 patients. Int J Radiat Oncol Biol Phys 43:795–803

Mehta MP, Paleologos NA, Mikkelsen T et al (2010) The role of chemotherapy in the management of newly diagnosed brain metastases: a systematic review and evidence-based clinical practice guideline. J Neurooncol 96:71–83

Narita Y, Shibui S (2009) Strategy of surgery and radiation therapy for brain metastases. Int J Clin Oncol 14:275–280

Neuhaus T, Ko Y, Muller RP, Grabenbauer GG et al (2009) A phase III trial of topotecan and whole brain radiation therapy for patients with CNS-metastases due to lung cancer. Br J Cancer 100:291–297

Ostermann S, Csajka C, Buclin T et al (2004) Plasma and cerebrospinal fluid pharmacokinetics of temozolomide in malignant glioma patients. Clin Cancer Res 10:3728–3736

Park YH, Park MJ, Ji SH et al (2009) Trastuzumab treatment improves brain metastasis outcomes through control and durable prolongation of systemic extracranial disease in HER2-over-expressing breast cancer patients. Br J Cancer 100:894–900

Patchell RA, Tibbs PA, Walsh JW et al (1990) A randomized trial of surgery in the treatment of single metastases to the brain. N Engl J Med 322:494–500

Robinet G, Thomas P, Breton JL et al (2001) Results of a phase III study of early versus delayed whole brain radiotherapy with concurrent cisplatin and vinorelbine combination in inoperable brain metastasis of non-small-cell lung cancer: Groupe Francais de Pneumo-Cancerologie (GFPC) Protocol 95–1. Ann Oncol 12:59–67

Sánchez Cos J, Sojo González MA et al (2009) Non-small cell lung cancer and silent brain metastasis. Survival and prognostic factors. Lung Cancer 63:140–145

Siena S, Crinò L, Danova M et al (2010) Dose-dense temozolomide regimen for the treatment of brain metastases from melanoma, breast cancer, or lung cancer not amenable to surgery or radiosurgery: a multicenter phase II study. Ann Oncol 21:655–661

Sneed PK, Lamborn KR, Forstner JM et al (1999) Radiosurgery for brain metastases: is whole brain radiotherapy necessary? Int J Radiat Oncol Biol Phys 43:949–958

Soffietti R, Ruda R, Mutani R (2002) Management of brain metastasis. J Neurol 249:1357–1369

Swinson BM, William FA (2008) Linear accelerator stereotactic radiosurgery for metastatic brain tumors: 17 years of experience at the University of Florida. Neurosurgery 62:1018–1032

Tsao MN, Lloyd NS, Wong RKS et al (2005) Radiotherapeutic management of brain metastases: a systematic review and meta-analysis. Cancer Treat Rev 31:256–273

Vecht CJ, Haaxma-Reiche H, Noordijk EM et al (1993) Treatment of single brain metastasis: radiotherapy alone or combined with neurosurgery. Ann Neurol 33:583–590

Walbert T, Gilbert MR (2009) The role of chemotherapy in the treatment of patients with brain metastases from solid tumors. Int J Clin Oncol 14:299–306

Weissman DE (1988) Glucocorticoid treatment for brain metastases and epidural spinal cord compression: a review. J Clin Oncol 6:543–551

Wilson CM, Gaber MW, Sabek OM et al (2009) Radiation-induced astrogliosis and blood-brain barrier damage can be abrogated using anti-TNF treatment. Int J Radiat Oncol Biol Phys 74:934–941

Wu C, Li YL, Wang ZM et al (2007) Gefitinib as palliative therapy for lung adenocarcinoma metastatic to the brain. Lung Cancer 57:359–364

Yuan H, Gaber MW, Boyd K et al (2006) Effects of fractionated radiation on the brain vasculature in a murine model: blood–brain barrier permeability, astrocyte proliferation, and ultrastructural changes. Int J Radiat Oncol Biol Phys 66:860–866

nature genetics

A genome-wide association study identifies two new susceptibility loci for lung adenocarcinoma in the Japanese population

Kouya Shiraishi[1], Hideo Kunitoh[2,13], Yataro Daigo[3,4], Atsushi Takahashi[5], Koichi Goto[6], Hiromi Sakamoto[7], Sumiko Ohnami[7], Yoko Shimada[1], Kyota Ashikawa[8], Akira Saito[9], Shun-ichi Watanabe[10], Koji Tsuta[11], Naoyuki Kamatani[5], Teruhiko Yoshida[7], Yusuke Nakamura[4], Jun Yokota[12], Michiaki Kubo[8] & Takashi Kohno[1]

Lung adenocarcinoma is the most common histological type of lung cancer, and its incidence is increasing worldwide. To identify genetic factors influencing risk of lung adenocarcinoma, we conducted a genome-wide association study and two validation studies in the Japanese population comprising a total of 6,029 individuals with lung adenocarcinoma (cases) and 13,535 controls. We confirmed two previously reported risk loci, 5p15.33 (rs2853677, $P_{combined} = 2.8 \times 10^{-40}$, odds ratio (OR) = 1.41) and 3q28 (rs10937405, $P_{combined} = 6.9 \times 10^{-17}$, OR = 1.25), and identified two new susceptibility loci, 17q24.3 (rs7216064, $P_{combined} = 7.4 \times 10^{-11}$, OR = 1.20) and 6p21.3 (rs3817963, $P_{combined} = 2.7 \times 10^{-10}$, OR = 1.18). These data provide further evidence supporting a role for genetic susceptibility in the development of lung adenocarcinoma.

Lung cancer is the leading cause of cancer-related death in most countries[1]. Lung cancer consists of three major histological types: adenocarcinoma, squamous-cell carcinoma and small-cell carcinoma[1–3]. Adenocarcinoma is the most common type, comprising ~40% of all cases of lung cancer, and its incidence is increasing in both Asian and Western countries. The development of lung adenocarcinoma is more weakly associated with smoking than are the developments of squamous and small-cell carcinomas, indicating that the mechanisms of carcinogenesis differ among these histological types. A better understanding of the genetic factors underlying the development of lung adenocarcinoma is strongly needed to elucidate the etiology of disease and identify high-risk individuals for targeted screening and/or prevention. In particular, the proportion of females and never smokers among patients with lung adenocarcinoma is considerably higher in Asians than in Europeans[2,3], suggesting that genetic factors contribute differently to disease in the two populations.

Genome-wide association studies (GWAS) of lung cancer with a full range of histological types have been conducted in European populations, and associations at 15q25.1, 5p15.33 and 6p21.33 have been identified[4–8]. Variants at these regions have been defined in European populations by a meta-analysis of GWAS according to histological types, and rs2736100 in *TERT* at 5p15.33 was found to be associated with risk of lung adenocarcinoma[9]. However, no additional loci reached genome-wide significance in the study; therefore, GWAS focusing on lung adenocarcinoma were greatly needed[9]. A recent GWAS on lung adenocarcinoma risk in the Japanese and Korean populations identified a new locus, 3q28 (*TP63*)[10]. Subsequently, a significant but weaker association of 3q28 variations with lung adenocarcinoma risk was validated in Europeans[11]. Notably, the association of this locus with cancer risk was supported by a recent GWAS on lung cancer with a full range of different histological types in the Chinese population[12]. These results indicate that there may be differences in the magnitude of the contribution of these loci to lung cancer susceptibility by ethnicity. Here, to further elucidate the genetic factors contributing to the development of lung adenocarcinoma, we performed a GWAS focusing on lung adenocarcinoma in the Japanese population and expanded the scale of our previous study in terms of both sample size and SNP coverage[10].

Using Illumina Omni1-Quad and OmniExpress chips, we genotyped 1,722 cases and 5,846 controls for 709,857 SNPs (**Supplementary Table 1**). Based on the results of a stringent quality-control analysis, we chose 538,166 autosomal SNPs, 1,695 cases and 5,333 control subjects for our GWAS analyses (Online Methods and

[1]Division of Genome Biology, National Cancer Center Research Institute, Tokyo, Japan. [2]Division of Thoracic Oncology, National Cancer Center Hospital, Tokyo, Japan. [3]Department of Medical Oncology, Shiga University of Medical Science, Shiga, Japan. [4]Laboratory of Molecular Medicine, Human Genome Center, Institute of Medical Science, University of Tokyo, Tokyo, Japan. [5]Laboratory for Statistical Analysis, Center for Genomic Medicine, RIKEN, Kanagawa, Japan. [6]Thoracic Oncology Division, National Cancer Center Hospital East, Chiba, Japan. [7]Division of Genetics, National Cancer Center Research Institute, Tokyo, Japan. [8]Laboratory for Genotyping Development, Center for Genomic Medicine, RIKEN, Kanagawa, Japan. [9]Statistical Genetics Analysis Division, StaGen Co. Ltd, Tokyo, Japan. [10]Division of Thoracic Surgery, National Cancer Center Hospital, Tokyo, Japan. [11]Division of Pathology and Clinical Laboratories, National Cancer Center Hospital, Tokyo, Japan. [12]Division of Multistep Carcinogenesis, National Cancer Center Research Institute, Tokyo, Japan. [13]Present address: Department of Respiratory Medicine, Mitsui Memorial Hospital, Tokyo, Japan. Correspondence should be addressed to T.K. (tkkohno@ncc.go.jp).

Received 21 February; accepted 18 June; published online 15 July 2012; doi:10.1038/ng.2353

Table 1 Summary of the GWAS and validation studies and the combined analyses

dbSNP locus	Gene	Allele [risk allele]	Stage	Cases Total	Cases RAF	Controls Total	Controls RAF	P^a	OR (95% CI)	P_{het}
rs2853677	*TERT*	T/C	GWAS	1,695	0.384	5,333	0.308	8.66×10^{-17}	1.41 (1.30–1.53)	
5p15.33	intron 2	[C]	First validation	2,955	0.374	7,036	0.297	8.62×10^{-21}	1.43 (1.32–1.54)	
			Second validation	1,373	0.360	1,132	0.290	5.88×10^{-6}	1.35 (1.19–1.54)	
			Combined validation[b]	4,328	0.370	8,168	0.296	3.90×10^{-25}	1.42 (1.32–1.50)	0.49
			Combined all[b]	6,023	0.374	13,501	0.300	2.80×10^{-40}	1.41 (1.32–1.50)	0.79
rs2736100	*TERT*	T/G	GWAS	1,695	0.458	5,329	0.391	7.31×10^{-12}	1.32 (1.22–1.42)	
5p15.33	intron 2	[G]	First validation	2,954	0.458	7,036	0.385	2.13×10^{-19}	1.39 (1.29–1.49)	
			Second validation	1,343	0.432	1,166	0.368	1.79×10^{-4}	1.27 (1.12–1.44)	
			Combined validation[b]	4,297	0.450	8,202	0.383	3.97×10^{-22}	1.36 (1.28–1.44)	0.22
			Combined all[b]	5,992	0.452	13,531	0.386	2.50×10^{-32}	1.34 (1.28–1.41)	0.39
rs10937405	*TP63*	C/T	GWAS	1,695	0.728	5,333	0.677	1.10×10^{-8}	1.29 (1.18–1.40)	
3q28	intron 1	[C]	First validation	2,953	0.714	7,036	0.663	9.22×10^{-10}	1.27 (1.18–1.37)	
			Second validation	1,375	0.704	1,166	0.682	1.22×10^{-1}	1.11 (0.97–1.26)	
			Combined validation[b]	4,328	0.711	8,202	0.666	8.17×10^{-10}	1.23 (1.15–1.31)	0.076
			Combined all[b]	6,023	0.715	13,535	0.670	6.92×10^{-17}	1.25 (1.19–1.32)	0.15
rs7216064	*BPTF*	A/G	GWAS	1,695	0.747	5,333	0.706	1.07×10^{-5}	1.22 (1.12–1.34)	
17q24.3	intron 9	[A]	First validation	2,955	0.736	7,036	0.708	7.72×10^{-5}	1.17 (1.08–1.27)	
			Second validation	1,376	0.744	1,166	0.708	4.70×10^{-3}	1.21 (1.06–1.39)	
			Combined validation[b]	4,331	0.739	8,202	0.708	1.34×10^{-6}	1.18 (1.10–1.26)	0.65
			Combined all[b]	6,026	0.741	13,535	0.707	7.40×10^{-11}	1.20 (1.13–1.26)	0.76
rs3817963	*BTNL2*	A/G	GWAS	1,695	0.363	5,331	0.327	5.54×10^{-5}	1.18 (1.09–1.28)	
6p21.3	intron 4	[G]	First validation	2,951	0.347	7,028	0.310	1.59×10^{-5}	1.18 (1.09–1.27)	
			Second validation	1,376	0.358	1,166	0.329	2.41×10^{-2}	1.16 (1.02–1.32)	
			Combined validation[b]	4,327	0.350	8,194	0.313	1.14×10^{-6}	1.17 (1.10–1.25)	0.86
			Combined all[b]	6,022	0.354	13,525	0.318	2.69×10^{-10}	1.18 (1.12–1.24)	0.97

RAF, risk allele frequency; P_{het}, *P* value for heterogeneity.
[a]Adjusted for age and gender. [b]The combined meta-analysis was performed using a fixed effect model.

Supplementary Fig. 1). We generated a quantile-quantile plot using the results of a logistic regression trend test (**Supplementary Fig. 1d**). The genomic inflation factor ($\lambda_{1,000}$)[13] was 1.021, indicating a low possibility of false-positive associations resulting from population stratification or genotype misclassification (**Supplementary Fig. 2**).

In the GWAS, two loci reached genome-wide significance for association ($P < 5 \times 10^{-8}$; **Supplementary Fig. 1e**); these two loci have been reported in previous GWAS (rs2736100 at 5p13.33 and rs10937405 at 3q28)[9,10]. We also identified a significant association for a SNP (rs2853677 at 5p13.33) that was not examined in our previous GWAS (**Table 1**). In addition, we examined associations of other previously reported loci with lung cancer risk (**Supplementary Table 2**). We found one locus (rs2131877 at 3q29)[14] to be associated with lung adenocarcinoma risk, but we could not confirm the associations between lung adenocarcinoma risk and the other loci identified in a recent GWAS of the European and Han Chinese populations[12]. These results are probably the result of the lower statistical power in our GWAS than in the previous GWAS (**Supplementary Table 2**). In addition, most of the earlier GWAS were performed in lung cancer representing a full range of histological types and in subjects of European descent. Therefore, differences in genetic modifiers and/or environmental factors in different histological types and populations might have contributed to the differing results.

To investigate additional susceptibility loci, we conducted a validation study using two independent sample sets consisting of 2,955 cases and 7,036 controls (first validation cohort) and 1,379 cases and 1,166 controls (second validation cohort) (**Supplementary Table 1**). Among 125 SNPs with a logistic regression trend of $P < 1 \times 10^{-4}$ in our GWAS, we selected 78 SNPs, excluding 38 SNPs within the same locus ($r^2 > 0.8$) and nine SNPs located at the previously reported loci, 5p13.33 and 3q28. We successfully genotyped all 78 SNPs in the first validation set using the multiplex PCR-based Invader assay, and 8 SNPs had ORs with a significance of $P < 0.05$ in the same direction of association (**Supplementary Table 3**). We then subjected these eight SNPs to the second validation set analysis. When we combined the results of both validation sets using a fixed effects model, two SNPs, rs7216064 at 17q24.3 and rs3817963 at 6p21.3, showed significant associations after Bonferroni correction ($P < 6.4 \times 10^{-4}$, calculated as 0.05/78) in addition to three SNPs at the two known loci described above (**Table 1**). When we combined the results of the GWAS and the validation study, both of the newly discovered loci reached genome-wide significance (rs7216064, $P = 7.4 \times 10^{-11}$, OR = 1.20; rs3817963, $P = 2.7 \times 10^{-10}$, OR = 1.18) (**Table 1**). The ORs were similar between the GWAS and the validation study, with no heterogeneity (**Table 1**). The strengths of the associations remained similar after adjustment for smoking (**Supplementary Table 4**). In a subgroup analysis (**Supplementary Table 5**), there was no clear association between the two newly discovered loci and gender or smoking behavior, and there was also no such association for the two known loci[10].

We next performed imputation analyses using the Japanese in Tokyo (JPT) and Han Chinese in Beijing (CHB) reference sets from the 1000 Genomes Project database (June 2010 release) (Online Methods), and we examined the associations between 1,665 putative SNPs and lung adenocarcinoma risk. We found a series of signals in high linkage disequilibrium (LD) with a marker SNP at 17q24.3 (rs7216064), and we observed significant associations with lung adenocarcinoma risk for 33 of the imputed SNPs (**Fig. 1a** and **Supplementary Table 6**). However, none of the SNPs in LD at 6p21.3 reached the *P* value of our marker SNP (**Fig. 1b**).

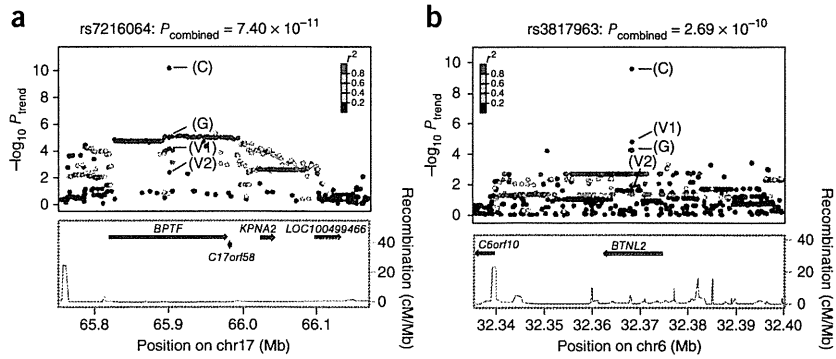

Figure 1 Regional plots of the identified marker SNPs. (**a**) rs7216064 at 17q24.3. (**b**) rs3817963 at 6p21.3. The marker SNP is shown in purple, and the r^2 values for the other SNPs are indicated by different colors. The correlations were estimated using data from the 1000 Genomes Project. The genes within the region of interest are annotated and are indicated by arrows. The blue lines indicate the recombination rates in cM per Mb. The $-\log_{10} P_{trend}$ values of the marker SNPs are shown for the GWAS (G), the first validation study (V1), the second validation study (V2) and the combined study (C).

SNP rs7216064 resides within intron 9 of *BPTF* (encoding bromodomain PHD finger transcription factor) at 17q24.3. Other imputed SNPs in this locus showing similarly significant associations were also synonymous (not resulting in amino acid changes in translated proteins). Based on the regional plot and recombination rates, we found that rs7216064 represented an LD region that includes three genes: *BPTF*, *C17orf58* (encoding a protein without known domains) and *KPNA2* (encoding karyopherin α 2) (**Fig. 1a**). Thus, to address the biological importance of 17q24.3 variants, we examined the mRNA expression levels of these three genes in 314 noncancerous lung tissues by real-time quantitative PCR (**Supplementary Note**). We detected expression of *BPTF*, but not of *C17orf58* or *KPNA2*, in these lung tissues. The expression of *BPTF* was marginally different depending on the genotype of the rs7216064 SNP ($P = 0.02$), implying low expression from the risk (G) allele (**Supplementary Table 7**). *BPTF* encodes a chromatin remodeling factor that regulates transcription through the specific recognition of methylated histone proteins[15]. Recently, chromatin remodeling genes have been implicated as tumor suppressors in lung[16] and other cancers[17]. Therefore, a low level of *BPTF* mRNA being associated with the risk allele might lead to an elevated risk for lung adenocarcinoma through decreased transcriptional regulation. However, further studies are needed to conclude whether *BPTF* is responsible for lung adenocarcinoma susceptibility.

SNP rs3817963 is located in intron 4 of *BTNL2* (encoding butyrophilin-like 2) at 6p21.3 (**Fig. 1b**). Based on the regional plot and recombination rates, rs3817963 represents an LD region that includes only a single gene, *BTNL2*. The top ten SNPs (genotyped or imputed), including rs3817963, were synonymous. The effects of the SNPs on the expression of *BTNL2* could not be assessed because of the low or absent expression of this gene in noncancerous lung tissues. *BTNL2* encodes a T cell co-stimulatory molecule, and associations between *BTNL2* SNPs and risk have been reported in several immune-related diseases, including asthma[18], vitiligo[19] and ulcerative colitis[20,21]. Therefore, *BTNL2* might affect lung adenocarcinoma risk by affecting immune responses against tumor cells. However, 6p21.3 is a part of the extended major histocompatibility complex (MHC) region, whose association with lung cancer risk has previously been reported[5]. The previously identified marker SNPs, rs3117582 and rs3131379, located 700 kb from the *BTNL2* locus, were monomorphic in our study populations. Therefore, it is possible that the association at 6p21.3 identified in the present study is not new, and further studies are warranted.

We here provide further evidence for the existence of genetic susceptibility in the development of lung adenocarcinoma through the identification of two candidate susceptibility loci, 17q24.3 and 6p21.3, at genome-wide significance. rs7216064 at 17q24.3 showed a tendency of association in the same direction as lung cancer risk in Europeans, although this association did not reach statistical significance, whereas rs3135353 at 6p21.3, which is in LD with rs3817963, showed a statistically significant association with lung cancer risk in European and American populations (**Supplementary Table 8**)[7,9]. Therefore, these loci might be involved in lung cancer risk in individuals of European descent. Further studies of these loci in multiple populations, including those with other histological types of lung cancers, will help to elucidate the etiology of lung adenocarcinoma.

URLs. The BioBank Japan project, http://biobankjp.org/; R, http://cran.r-project.org/; PLINK statistical software v1.06, http://pngu.mgh.harvard.edu/~purcell/plink/; Primer3 v0.3.0, http://frodo.wi.mit.edu/primer3/; UCSC Genome Browser, http://genome.ucsc.edu/; LocusZoom, http://csg.sph.umich.edu/locuszoom/; a catalog of genome-wide association studies, http://www.genome.gov/gwastudies/; SNPinfo Web Server, http://manticore.niehs.nih.gov/index.html; Illumina's IconDB resource, http://www.illumina.com/science/icontroldb.ilmn.

METHODS

Methods and any associated references are available in the online version of the paper.

Note: Supplementary information is available in the online version of the paper.

ACKNOWLEDGMENTS

We thank all of the subjects for participating in the study, and we also thank the collaborating physicians for assisting with sample collection. We are grateful to the members of BioBank Japan, the National Cancer Center Biobank and the Rotary Club of Osaka-Midosuji District 2660 Rotary International in Japan for supporting our study. We thank Y. Aoi, T. Odaka, M. Okuyama, H. Totsuka, S. Chiku, A. Kuchiba and the technical staff of the Center for Genome Medicine, National Cancer Center Research Institute, for providing technical and methodological assistance. We also thank H. Hirose of Health Center, Keio University and D. Saito of National Cancer Center Hospital (present affiliation: Nihonbashi Daizo Clinic) for DNA samples of control subjects. This work was supported in part by Grants-in-Aid from the Ministry of Health, Labor and Welfare for Research on Applying Health Technology and for the 3rd-term Comprehensive 10-year Strategy for Cancer Control; from the Ministry of Education, Culture, Sports, Science and Technology of Japan for Scientific Research on Innovative Areas (22131006); from the Japan Society for the Promotion of Science for Research Activity Start-up (23800073) and for Young Scientists (B) (24790340); and by the National Cancer Center Research and Development Fund. This work was also conducted as a part of the BioBank Japan Project supported by the Ministry of Education, Culture, Sports, Science and Technology, Japan. The National Cancer Center Biobank is supported by the National Cancer Center Research and Development Fund, Japan.

AUTHOR CONTRIBUTIONS

K.S., J.Y., M.K. and T.K. designed the study. A.T., K.A., S.O., N.K. and A.S. analyzed the GWAS and replication study. H.S., Y.S., T.Y. and K.S. performed the genotyping for the GWAS and the replication study. H.K., K.G., S.W. and K.T. recruited

subjects and participated in diagnostic evaluations. K.S. and T.K. wrote the manuscript. M.K., Y.D., T.Y. and Y.N. contributed to the overall GWAS design.

COMPETING FINANCIAL INTERESTS
The authors declare no competing financial interests.

Published online at http://www.nature.com/doifinder/10.1038/ng.2353.
Reprints and permissions information is available online at http://www.nature.com/reprints/index.html.

1. Colvy, T.V. *et al.* Adenocarcinoma. in *World Health Organization Classification of Tumors: Pathology and Genetics, Tumours of Lung, Pleura, Thymus and Heart* (eds. Travis, W.D., Brambilla, E., Muller-Hermelink, H.K. & Harris, C.C.) 35–44 (IARC Press, Lyon, France, 2004).
2. Subramanian, J. & Govindan, R. Lung cancer in never smokers: a review. *J. Clin. Oncol.* **25**, 561–570 (2007).
3. Sun, S., Schiller, J.H. & Gazdar, A.F. Lung cancer in never smokers—a different disease. *Nat. Rev. Cancer* **7**, 778–790 (2007).
4. Broderick, P. *et al.* Deciphering the impact of common genetic variation on lung cancer risk: a genome-wide association study. *Cancer Res.* **69**, 6633–6641 (2009).
5. Wang, Y. *et al.* Common 5p15.33 and 6p21.33 variants influence lung cancer risk. *Nat. Genet.* **40**, 1407–1409 (2008).
6. McKay, J.D. *et al.* Lung cancer susceptibility locus at 5p15.33. *Nat. Genet.* **40**, 1404–1406 (2008).
7. Hung, R.J. *et al.* A susceptibility locus for lung cancer maps to nicotinic acetylcholine receptor subunit genes on 15q25. *Nature* **452**, 633–637 (2008).
8. Amos, C.I. *et al.* Genome-wide association scan of tag SNPs identifies a susceptibility locus for lung cancer at 15q25.1. *Nat. Genet.* **40**, 616–622 (2008).
9. Landi, M.T. *et al.* A genome-wide association study of lung cancer identifies a region of chromosome 5p15 associated with risk for adenocarcinoma. *Am. J. Hum. Genet.* **85**, 679–691 (2009).
10. Miki, D. *et al.* Variation in *TP63* is associated with lung adenocarcinoma susceptibility in Japanese and Korean populations. *Nat. Genet.* **42**, 893–896 (2010).
11. Wang, Y. *et al.* Variation in *TP63* is associated with lung adenocarcinoma in the UK population. *Cancer Epidemiol. Biomarkers Prev.* **20**, 1453–1462 (2011).
12. Hu, Z. *et al.* A genome-wide association study identifies two new lung cancer susceptibility loci at 13q12.12 and 22q12.2 in Han Chinese. *Nat. Genet.* **43**, 792–796 (2011).
13. Freedman, M.L. *et al.* Assessing the impact of population stratification on genetic association studies. *Nat. Genet.* **36**, 388–393 (2004).
14. Yoon, K.A. *et al.* A genome-wide association study reveals susceptibility variants for non-small cell lung cancer in the Korean population. *Hum. Mol. Genet.* **19**, 4948–4954 (2010).
15. Ruthenburg, A.J. *et al.* Recognition of a mononucleosomal histone modification pattern by BPTF via multivalent interactions. *Cell* **145**, 692–706 (2011).
16. Medina, P.P. & Sanchez-Cespedes, M. Involvement of the chromatin-remodeling factor BRG1/SMARCA4 in human cancer. *Epigenetics* **3**, 64–68 (2008).
17. Wilson, B.G. & Roberts, C.W. SWI/SNF nucleosome remodellers and cancer. *Nat. Rev. Cancer* **11**, 481–492 (2011).
18. Hirota, T. *et al.* Genome-wide association study identifies three new susceptibility loci for adult asthma in the Japanese population. *Nat. Genet.* **43**, 893–896 (2011).
19. Jin, Y. *et al.* Variant of *TYR* and autoimmunity susceptibility loci in generalized vitiligo. *N. Engl. J. Med.* **362**, 1686–1697 (2010).
20. Asano, K. *et al.* A genome-wide association study identifies three new susceptibility loci for ulcerative colitis in the Japanese population. *Nat. Genet.* **41**, 1325–1329 (2009).
21. Anderson, C.A. *et al.* Meta-analysis identifies 29 additional ulcerative colitis risk loci, increasing the number of confirmed associations to 47. *Nat. Genet.* **43**, 246–252 (2011).

BRIEF COMMUNICATIONS

nature medicine

KIF5B-RET fusions in lung adenocarcinoma

Takashi Kohno[1,15], Hitoshi Ichikawa[2,15], Yasushi Totoki[3], Kazuki Yasuda[4], Masaki Hiramoto[4], Takao Nammo[4], Hiromi Sakamoto[2], Koji Tsuta[5], Koh Furuta[5], Yoko Shimada[1], Reika Iwakawa[6], Hideaki Ogiwara[1], Takahiro Oike[6], Masato Enari[7], Aaron J Schetter[8], Hirokazu Okayama[6,8], Aage Haugen[9], Vidar Skaug[9], Suenori Chiku[10], Itaru Yamanaka[11], Yasuhito Arai[3], Shun-ichi Watanabe[12], Ikuo Sekine[13], Seishi Ogawa[14], Curtis C Harris[8], Hitoshi Tsuda[5], Teruhiko Yoshida[2], Jun Yokota[6] & Tatsuhiro Shibata[3]

We identified in-frame fusion transcripts of *KIF5B* (the kinesin family 5B gene) and the *RET* oncogene, which are present in 1–2% of lung adenocarcinomas (LADCs) from people from Japan and the United States, using whole-transcriptome sequencing. The *KIF5B-RET* fusion leads to aberrant activation of RET kinase and is considered to be a new driver mutation of LADC because it segregates from mutations or fusions in *EGFR*, *KRAS*, *HER2* and *ALK*, and a RET tyrosine kinase inhibitor, vandetanib, suppresses the fusion-induced anchorage-independent growth activity of NIH3T3 cells.

A considerable proportion of LADCs, the most common histological type of lung cancer that comprises ~40% of the total cases, develops through activation of oncogenes, for example, somatic mutations in *EGFR* (10–50% of cases) or *KRAS* (10–30% of cases) or fusion of *ALK* (5% of cases), in a mutually exclusive manner[1–4]. Tyrosine kinase inhibitors (TKIs) targeting the EGFR and ALK proteins are effective in the treatment of LADCs that carry *EGFR* mutations and *ALK* fusions[1–3], respectively.

We performed whole-transcriptome sequencing (RNA sequencing)[5] of 30 LADC specimens from Japanese individuals to identify new chimeric fusion transcripts that could be targets for therapy[3,5,6]. These LADCs were 2 carcinomas with *EML4-ALK* fusions, 4 with *EGFR* or *KRAS* mutations and 24 without these fusions or mutations (**Supplementary Table 1**). Identifying candidate fusions represented by >20 paired-end reads and validation by Sanger sequencing of the RT-PCR products (**Supplementary Methods**) led to the identification of seven fusion transcripts, including *EML4-ALK* (**Supplementary Table 1**). We detected one of these fusions between *KIF5B* on chromosome 10p11.2 and *RET* on chromosome 10q11.2 in subject BR0020 (**Fig. 1** and **Supplementary Fig. 1a**). We then further investigated this fusion, as fusions between *RET* and genes other than *KIF5B* have previously been shown to drive papillary thyroid tumor formation[6,7].

RT-PCR and a Sanger sequencing analysis of 319 LADC specimens from Japanese individuals (**Supplementary Table 2**), including 30 that had been subjected to whole-transcriptome sequencing, revealed that 1.9% (6 out of 319) expressed *KIF5B-RET* fusion transcripts (**Fig. 1b** and **Supplementary Fig. 1b**). We identified four variants in these six tumors, and all of these variants were in frame (**Fig. 1a**).

A genomic PCR analysis of the six tumors that were positive for RET fusions revealed somatic fusions of the *KIF5B* introns 15, 16, 23 or 24 at chromosome 10p11.2 with the *RET* introns 7 or 11 at 10q11.2 (**Supplementary Fig. 1c,d**), indicating that a chromosomal inversion had occurred between the long and short arms in the centromeric region of chromosome 10 (**Supplementary Figs. 1e** and **2**). We verified this chromosomal inversion using fluorescence *in situ* hybridization, which revealed a split in the signals for the probes that flank the *RET* translocation sites in tumors positive for the *KIF5B-RET* fusion (**Supplementary Fig. 2**).

The tumors positive for the *KIF5B-RET* fusion were all well or moderately differentiated (**Table 1** and **Supplementary Fig. 3**). None of the subjects with these tumors had a history of thyroid cancer, and none showed abnormal findings in their thyroid tissues as determined by computed tomography or positron emission tomography before surgery for LADC. All five examined tumors with the *KIF5B-RET* fusion were positive for thyroid transcription factor 1 (TTF-1) and napsin A aspartic proteinase (Napsin A)[8] but were negative for thyroglobulin[9], indicating that they were of pulmonary origin (**Table 1** and **Supplementary Fig. 3**). The LADCs that were positive for the *KIF5B-RET* fusion showed twofold to 30-fold higher *RET* expression than non-cancerous lung tissues (**Fig. 1b** and **Supplementary Figs. 4** and **5**). An immunohistochemical analysis using an antibody against the C-terminal region of the RET protein detected positive cytoplasmic staining in the tumor cells of the fusion-positive LADCs (**Table 1** and **Supplementary Fig. 3b**) but did not detect this staining in any of the non-cancerous lung cells. A western blot analysis confirmed the expression of the fusion proteins in the LADCs (**Supplementary Fig. 6**).

To address the prevalence of *KIF5B-RET* fusions in LADCs from individuals of non-Asian ancestry, we examined LADCs in cohorts from the United States and Norway (**Supplementary Table 2**). We detected a fusion transcript in 1 of the 80 (1.3%) subjects from the

[1]Division of Genome Biology, National Cancer Center Research Institute, Chuo-ku, Tokyo, Japan. [2]Division of Genetics, National Cancer Center Research Institute, Chuo-ku, Tokyo, Japan. [3]Division of Cancer Genomics, National Cancer Center Research Institute, Chuo-ku, Tokyo, Japan. [4]Department of Metabolic Disorder, Diabetes Research Center, Research Institute, National Center for Global Health and Medicine, Shinjuku-ku, Tokyo, Japan. [5]Division of Pathology and Clinical Laboratories, National Cancer Center Hospital, Chuo-ku, Tokyo, Japan. [6]Division of Multistep Carcinogenesis, National Cancer Center Research Institute, Chuo-ku, Tokyo, Japan. [7]Division of Refractory Cancer Research, National Cancer Center Research Institute, Chuo-ku, Tokyo, Japan. [8]Laboratory of Human Carcinogenesis, Center for Cancer Research, National Cancer Institute, US National Institutes of Health, Bethesda, Maryland, USA. [9]Section of Toxicology, Department of Chemical and Biological Working Environment, National Institute of Occupational Health, Oslo, Norway. [10]Science Solutions Division, Mizuho Information and Research Institute, Chiyoda-ku, Tokyo, Japan. [11]Statistical Genetics Analysis Division, StaGen, Taito-ku, Tokyo, Japan. [12]Division of Thoracic Surgery, National Cancer Center Hospital, Chuo-ku, Tokyo, Japan. [13]Division of Thoracic Oncology, National Cancer Center Hospital, Chuo-ku, Tokyo, Japan. [14]Cancer Genomics Project, University of Tokyo, Bunkyo-ku, Tokyo, Japan. [15]These authors equally contributed to this work. Correspondence should be addressed to T.K. (tkkohno@ncc.go.jp).

Received 23 August 2011; accepted 16 December 2011; published online 12 February 2012; doi:10.1038/nm.2644

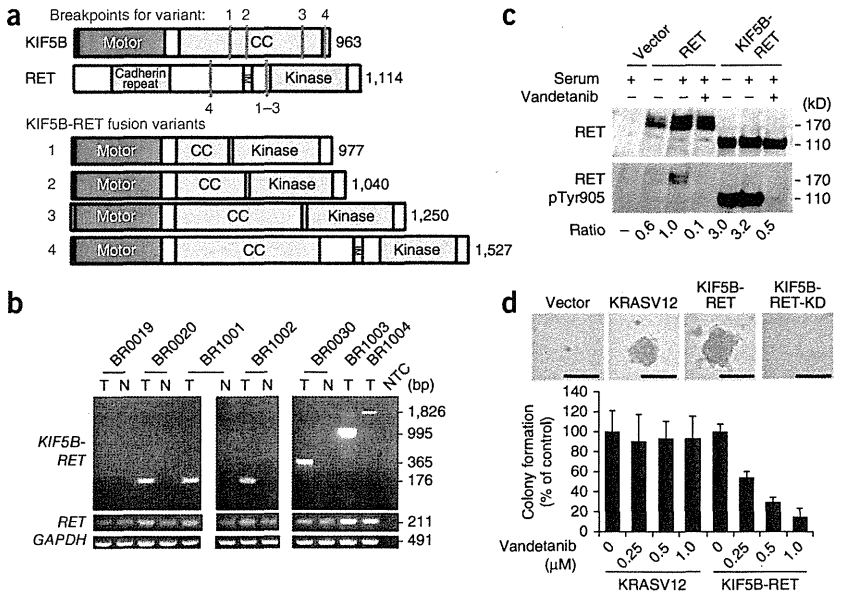

Figure 1 *KIF5B-RET* fusions in LADC. (**a**) Schematic representations of the wild-type KIF5B and RET proteins as well as the four fusion variants identified in this study. The breakpoints for each variant are indicated with red lines. CC, coiled coil; TM, transmembrane. (**b**) Detection of *KIF5B-RET* fusions by RT-PCR. RT-PCR products for the *RET* kinase domain (exons 12 and 13) and *GAPDH* are shown below. Six LADCs positive for *KIF5B-RET* fusions (T) are shown, with four corresponding non-cancerous lung tissues (N), a no-template control (NTC) and one LADC that was negative for the fusion (BR0019). (**c**) Activation of RET kinase activity in the KIF5B-RET protein and the suppression of this activity by vandetanib. H1299 lung cancer cells were transfected with an empty vector, wild-type RET (RET) or KIF5B-RET expression plasmids and treated either with DMSO (serum) or vandetanib, as indicated. The ratios of phosphorylated Tyr905 (pTyr905) RET to total RET signals with respect to wild-type RET after the serum treatment are listed below the gels. (**d**) Anchorage-independent growth of NIH3T3 cells expressing KIF5B-RET protein and the suppression of this growth by vandetanib. Representative pictures of colonies without vandetanib treatment (top). Scale bars, 50 μm. Bar graph showing the percentage (± s.d.) of colonies formed after treatment with the indicated amounts of vandetanib (average results of three independent experiments) with respect to those formed by DMSO-treated cells. The study was approved by the institutional review boards of institutions participating in this study.

United States (an individual of European ancestry) (**Supplementary Fig. 7**), but we detected no fusion transcripts in the 34 subjects from Norway (**Supplementary Table 3**); *KIF5B-RET* fusions occurred in 1–2% of LADCs in both Asians and non-Asians. The individual from the United States with the *RET* fusion was classified as an 'ever smoker', whereas the six individuals from Japan with the *RET* fusion were 'never smokers' (**Table 1**). Therefore, prevalence of LADC with regard to smoking status is unclear. We did not detect the *KIF5B-RET* fusion in other major subtypes of lung cancer, including 234 squamous-cell, 17 large-cell and 20 small-cell lung carcinomas (**Supplementary Table 3**). The fusion was also not present in other types of adenocarcinomas, including those of the ovary ($n = 100$) and colon ($n = 200$) (data not shown), suggesting that it is specific to LADC.

All seven subjects with LADC harboring the *KIF5B-RET* fusion were negative for *EGFR*, *KRAS* and *ALK* mutations or fusions and were negative for mutations in *HER2*, which is an additional driver mutation in LADC[10] (**Table 1** and **Supplementary Table 4**). The mutually exclusive nature of the *RET* fusions and other oncogenic alterations[1,2,11] suggests that the *KIF5B-RET* fusion is a driver mutation. All proteins encoded by the four *KIF5B-RET* fusion variants contained the KIF5B coiled-coil domain, which functions in protein dimerization[12], and retained the full RET kinase domain, similar to other types of oncogenic *RET* fusions observed in thyroid tumors (**Fig. 1a**)[13]. The KIF5B-RET proteins are likely to form a homodimer through the coiled-coil domain of KIF5B, causing an aberrant activation of the kinase function of RET in a manner similar to the *PTC-RET* and *KIF5B-ALK* fusions[7,14]. In fact, the N-terminal portion of the KIF5B coiled-coil region, which is retained in all variants, has been predicted to have the ability to dimerize through two coiled-coil structures[15]. Consistently, when the *KIF5B-RET* variant 1 was exogenously expressed in H1299 human lung cancer cells without wild-type or fusion *RET* expression, Tyr905, which is located in the activation loop of the RET kinase site[15,16], was phosphorylated in the absence of serum stimulation, indicating an aberrant activation of *RET* kinase[16,17] by fusion with *KIF5B* (**Fig. 1c**). This phosphorylation was suppressed by vandetanib, a TKI against RET (as well as other tyrosine kinases, including EGFR and VEGFR)[18] (**Fig. 1c** and **Supplementary Fig. 8**).

Expression of exogenous *KIF5B-RET*, but not *KIF5B-RET*-KD (a kinase-dead mutant corresponding to S765P in wild-type RET[17]), induced morphological transformation (**Supplementary Fig. 9**) and anchorage-independent growth of NIH3T3 fibroblasts in a way that was analogous to the induction caused by mutant *KRAS* (KRASV12) (**Fig. 1d**). Consistently, phosphorylation of Tyr905 was higher in the KIF5B-RET

Table 1 Characteristics of lung adenocarcinomas with the *KIF5B-RET* fusion

Sample	Country	Sex	Age[a]	Smoking	*KIF5B-RET* fusion[b]	Pathological stage	Pathological findings	RET staining	TTF-1 staining	Napsin A staining	Thyroglobulin staining
BR0020	Japan	Male	57	Never	K15; R12 (variant 1)	IIB	Moderately differentiated ADC	+	+	+	−
BR1001	Japan	Female	65	Never	K15; R12 (variant 1)	IB	Well differentiated ADC	+	+	+	−
BR1002	Japan	Female	64	Never	K15; R12 (variant 1)	IB	Well differentiated ADC	+	+	+	−
BR0030	Japan	Male	57	Never	K16; R12 (variant 2)	IA	Well differentiated ADC	+	+	+	−
BR1003	Japan	Male	28	Never	K23; R12 (variant 3)	IA	Well differentiated ADC	+	+	+	−
BR1004	Japan	Female	71	Never	K24; R8 (variant 4)	IA	Moderately differentiated ADC	NT	NT	NT	NT
NCI1580	USA	Male	63	Ever[c]	K15; R12 (variant 1)	II	Moderately differentiated ADC	NT	NT	NT	NT

[a]Age in years. [b]Fused exon numbers of *KIF5B* (K) and *RET* (R); and variant types (in parentheses) are shown. None of the subjects had oncogenic *EGFR*, *KRAS*, *HER2* or *ALK* mutations or fusions. [c]The number of pack years smoked for this subject is not known. NT, not tested.